Journal of Medicinal Chemistry

Article

pubs.acs.org/jmc

Structure-Guided Design, Synthesis, and Evaluation of Guanine-Derived Inhibitors of the eIF4E mRNA−Cap Interaction†

Xiaoqi Chen,*[,‡] David J. Kopecky,[‡] Jeff Mihalic,[‡] Shawn Jeffries,[∥] Xiaoshan Min,[§] Julie Heath,[‡] Jeff Deignan,[‡] SuJen Lai,[‡] Zice Fu,[‡] Cristiano Guimaraes,[§] Shanling Shen,[∥] Shyun Li,[∥] Sheree Johnstone,[§] Stephen Thibault,[§] Haoda Xu,[§] Mario Cardozo,[§] Wang Shen,[‡] Nigel Walker,[§] Frank Kayser,[‡] and Zhulun Wang*[,§]

[‡]Department of Chemistry Research & Discovery, [§]Department of Molecular Structure, [∥]Department of Oncology, Amgen Inc., 1120 Veterans Boulevard, South San Francisco, California 94080, United States

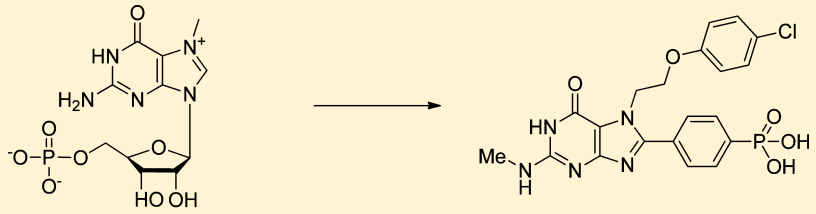

ABSTRACT: The eukaryotic initiation factor 4E (eIF4E) plays a central role in the initiation of gene translation and subsequent protein synthesis by binding the 5′ terminal mRNA cap structure. We designed and synthesized a series of novel compounds that display potent binding affinity against eIF4E despite their lack of a ribose moiety, phosphate, and positive charge as present in m7-GMP. The biochemical activity of compound **33** is 95 nM for eIF4E in an SPA binding assay. More importantly, the compound has an IC_{50} of 2.5 μM for inhibiting cap-dependent mRNA translation in a rabbit reticular cell extract assay (RRL-IVT). This series of potent, truncated analogues could serve as a promising new starting point toward the design of neutral eIF4E inhibitors with physicochemical properties suitable for cellular activity assessment.

INTRODUCTION

Unregulated cell growth is the hallmark of aggressive metastatic cancer.[1] Traditional cytotoxic chemotherapy has attempted to halt this growth by targeting the fundamental process of DNA replication with limited success. A clinically unexplored avenue for therapeutic intervention is the essential cellular process of protein synthesis.[2,3]

Protein translation requires the coordinated action of multiple cytoplasmic ribonucleic acid protein complexes and is tightly regulated by mitogenic signal transduction pathways.[4] Translation initiation is regarded as the rate-limiting step in new protein synthesis. Initiation proceeds through the recognition of methyl-7-guanosine (m^7GpppN or cap) at the 5′ end of all nuclear encoded mRNAs by the cap binding protein eIF4E. Once formed, the eIF4E/mRNA complex then binds to the scaffolding protein eIF4G and the helicase eIF4A forming the eIF4F complex, which is then recruited to ribosomal subunits where translation ensues.[5]

eIF4E is overexpressed in a wide variety of malignant cell lines and primary human tumors such as carcinomas of the breast,[6] colon,[7] and head and neck,[8] non-Hodgkin's lymphomas,[9] and chronic and acute M4/M5 myelogenous leukemias.[10] mRNA transcripts that are most profoundly influenced by activation of eIF4E typically include growth promoting factors and proto-oncogenes such as cMyc, Ornithine decarboxylase, Cyclin D1, and VEGF.[11−15] These mRNAs are characterized by having highly structured 5′ UTR regions that generally inhibit translation. The elevated level of eIF4E in tumor tissue selectively facilitates translation of these messages while leaving translation of bulk mRNAs unchanged. Activation of eIF4E lies most downstream on the axis of growth factor signaling through the PI3K−Akt−mTor pathway; signaling via this network is frequently upregulated during human tumorigenesis.[16] Inhibition of cap-dependent translation by the ectopic expression of the eIF4E repressor protein, 4E binding protein 1, reduces breast cancer tumorgenicity and resistance to apoptosis.[17] Additionally, the development of eIF4E-specific antisense oligonucleotides (ASOs) modified to enhance their tissue stability and nuclease resistance required for systemic anticancer therapy were reported. The impact of eIF4E reduction in normal tissues was assessed. Despite reducing eIF4E levels by 80% in mouse liver, eIF4E-specific ASO administration did not affect body weight, organ weight, or liver transaminase levels, thereby providing the first *in vivo* evidence that cancer may be more susceptible to eIF4E inhibition than normal tissues.[18] The above research results generated renewed interest in finding small molecule inhibitors of the eIF4E mRNA-cap interaction suitable for probing the role of cap dependent translation in cancer biology.

Received: January 11, 2012
Published: March 29, 2012

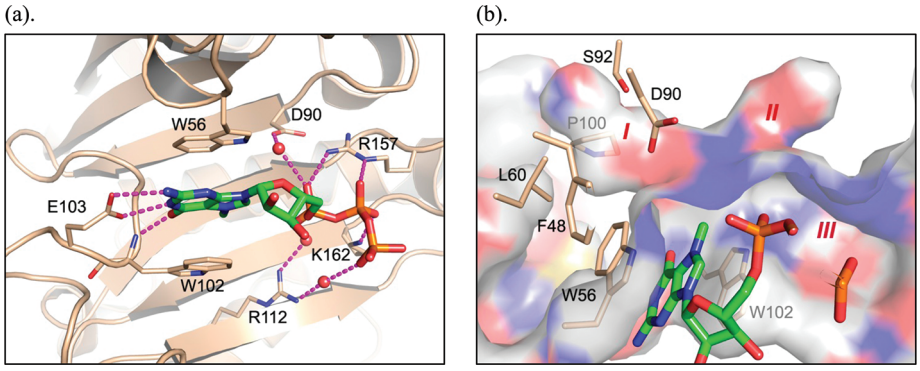

Figure 1. m7-GTP binding to eIF4E (PDB code: 1IPC). (a) Ribbon representation of the m7-GTP binding in the cap-binding slot of eIF4E with selected residues shown as sticks. Both eIF4E and m7-GTP are colored by element with carbon atoms in beige in the protein and green in m7-GTP, oxygen atoms in red, nitrogen atoms in blue, and phosphorus atoms in orange. (b) Molecular surface representation of pockets I, II, and III in the cap-binding site: (I) pronounced lipophilic pocket adjacent and perpendicular to the guanosine moiety formed by residues Phe48, Trp56, Leu60, Pro100, Ser92, and Asp90; (II) small pocket formed by residues Arg112, Leu114, Val153, Asn155, Ala164, and Trp166; (III) phosphate binding pocket.

As part of our efforts aimed at developing small molecule inhibitors of eIF4E, a high-throughput screen (HTS) of our in-house small molecule library was conducted. However, no *bona fide* leads were identified from these screening efforts. Given the attractiveness of the target and the availability of cocrystal structures of eIF4E in complex with the cap analogues m7-GDP, m7-GTP, and m7-GpppA as well as with m7-GpppA and the 4E-BP1 fragment,[19−23] we embarked on a structure based design approach to identify novel small molecule eIF4E inhibitors.

Analogues of the mRNA cap have been useful in studying eIF4E function and cap-dependent translation. Previously, several N7-substituted guanosine nucleoside and nucleotide analogues were evaluated for their ability to inhibit eIF4E binding to 7-methyl GTP.[24−28] Further analysis of the eIF4E cocrystal structures with cap analogues revealed that a unique hydrophobic pocket presents itself adjacent to the guanosine moiety. Our strategy was to first optimize the N7 position of m7-GMP directed toward binding in this pocket and subsequently investigate the other parts of these N7-alkyl GMP analogues. We successfully discovered a series of 7-alkyl guanosine nucleotide analogues as well as 7-alkyl guanosine phosphonic acid analogues which demonstrated high binding affinity for eIF4E. This report describes the structured-guided medicinal chemistry efforts toward these novel eIF4E cap binding antagonists as well as the cocrystal structures of these compounds in complex with eIF4E.

RESULTS AND DISCUSSION

Various cocrystal structures of human eIF4E in complex with cap analogues, including m7-GDP, m7-GTP, and m7-GpppA as well as the ternary complex of eIF4E with m7-GpppA in the presence of the 4E-BP1 fragment, have been reported.[20−23] All of the structures reveal that these cap analogues bind in a narrow cap-binding slot on the protein's concave surface. The delocalized positively charged 7-methyl guanosine ring forms cation-π interactions with Trp102 and Trp56 through being sandwiched between these two conserved tryptophans (Figure 1a). Here, the delocalized positive charge makes a large contribution to their binding affinity to eIF4E. The binding potency of GpppG compared with m7-GpppG is 276-fold lower against eIF4E. In addition, the carbonyl group of the guanine engages in a hydrogen bond interaction with the backbone amide of Trp102. N1 and N2 are also engaged in hydrogen bond contacts with Glu103. It appears that structural changes in these regions would not be favorable, as it would disrupt these key H-bond interactions. Furthermore, the phosphate moiety also makes a large contribution to the binding affinity of m7-GTP to the eIF4E protein. The triphosphate moiety forms an extensive hydrogen-bonding network through water molecules with Arg112, Arg157, and Lys162. The k_i of m7-GTP against eIF4E was 28 nM, determined in the protein binding assay. Compared to the case of m7-GTP, m7-GDP and m7-GMP's binding affinities against eIF4E were reduced by 39- and 407-fold, respectively. While both the m7-guanosine and phosphate moieties make important contributions for the binding of the cap analogues to eIF4E, the ribose ring is positioned at the entrance of the cap-binding side. The 3- and 4-hydroxy moieties on the ribose ring point toward the solvent and do not participate in any specific interactions with the protein. While analyzing the interactions of m7-GTP analogues with eIF4E, we were intrigued by the pronounced lipophilic pocket adjacent and perpendicular to the guanosine moiety formed by Phe48, Leu60, Pro100, Ser92, and Asp90 (pocket I, Figure 1b). We envisioned targeting this pocket to increase the binding affinity of N7-modified GMP analogues, thus compensating for the loss from β- and γ-phosphate groups in regard to m7-GTP.

A number of analogues were synthesized by alkylation of guanine monophosphate, as shown in Scheme 1. The SAR results are summarized in Table 1.

In agreement with previous reports, the N7-benzyl analogue **2** showed similar binding affinity as m7-GMP **1**. We were delighted to find that when guanine monophosphate was alkylated with a Cl-phenylpropyl group, a derivative with

Scheme 1. General Synthesis of N7-Modified GMP Analogues

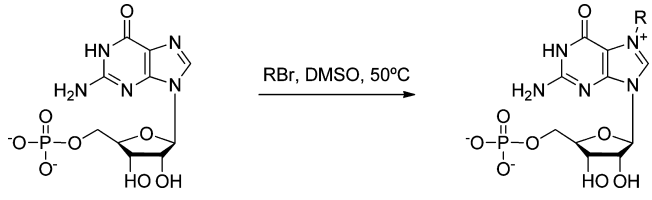

dx.doi.org/10.1021/jm300037x | J. Med. Chem. 2012, 55, 3837−3851

Table 1. SAR of N7-Substituted GMP Analogues

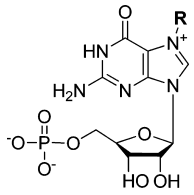

Compound	Structure	SPA IC_{50} (μM)	RRL-IVT IC_{50} (μM)	Compound	Structure	SPA IC_{50} (μM)	RRL-IVT IC_{50} (μM)
1		14	39	**9**	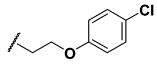	0.059±0.02(n=4)	1.9
2		15.5	26.8	**10**	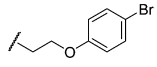	0.041±0.02(n=3)	0.7
3	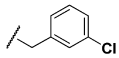	56.8±35.3	-	**11**	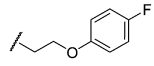	1.59	22
4		54.5	-	**12**	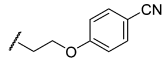	0.125	1.5
5	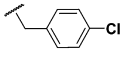	10±2.96(n=3)	49.8	**13**	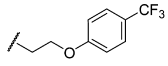	2.57	-
6	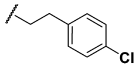	49.3	21.1	**14**	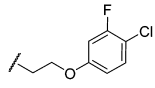	0.056±0.01	2.65
7	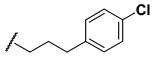	5.35	-	**15**	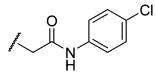	85.4	-
8	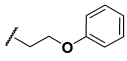	43±22.1(n=2)	48.3±0.007(n=2)	**16**	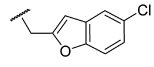	0.117	4.3

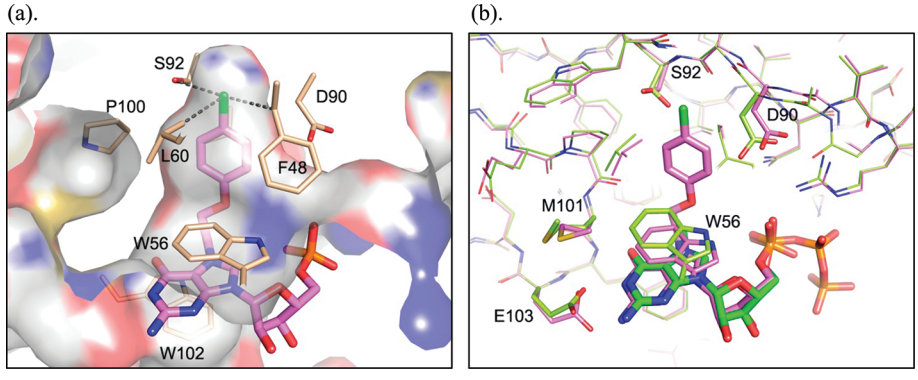

Figure 2. Cocrystal structure of eIF4E in complex with compound **9**. (a) Binding mode of compound **9** in the cap-binding slot in eIF4E. The protein is shown as a molecular surface representation. The selected residues involved in interactions with **9** are shown as sticks. The color code is the same as that in Figure 1, except that the carbon atoms in compound **9** are colored in magenta. (b) Overlay of the cocrystal structures of compound **9** and m7-GTP (PDB code: 1IPC) with eIF4E.

improved binding potency for eIF4E was obtained (**7** vs **1**). Encouraged by this result we further probed the binding pocket. Interestingly and quite unexpectedly, the Cl-phenoxyethyl derivative **9** demonstrated significantly improved binding potency for eIF4E, with an IC_{50} of ∼60 nM. This constitutes a remarkable 200-fold increase in potency over m7-GMP and an almost 100-fold increase over that of the unsubstituted phenoxyethyl derivative **8**. Similarly enhanced binding affinities were observed for the 4-cyano and 4-bromo phenoxyethyl derivatives **10** and **12**, while the fluoro- and trifluorometyl derivatives **11** and **13** only showed a moderate 20−30-fold increase in affinity over the unsubstituted phenoxyethyl

dx.doi.org/10.1021/jm300037x | J. Med. Chem. 2012, 55, 3837−3851

Scheme 2. General Synthesis of Deazaguanine Analogues[a]

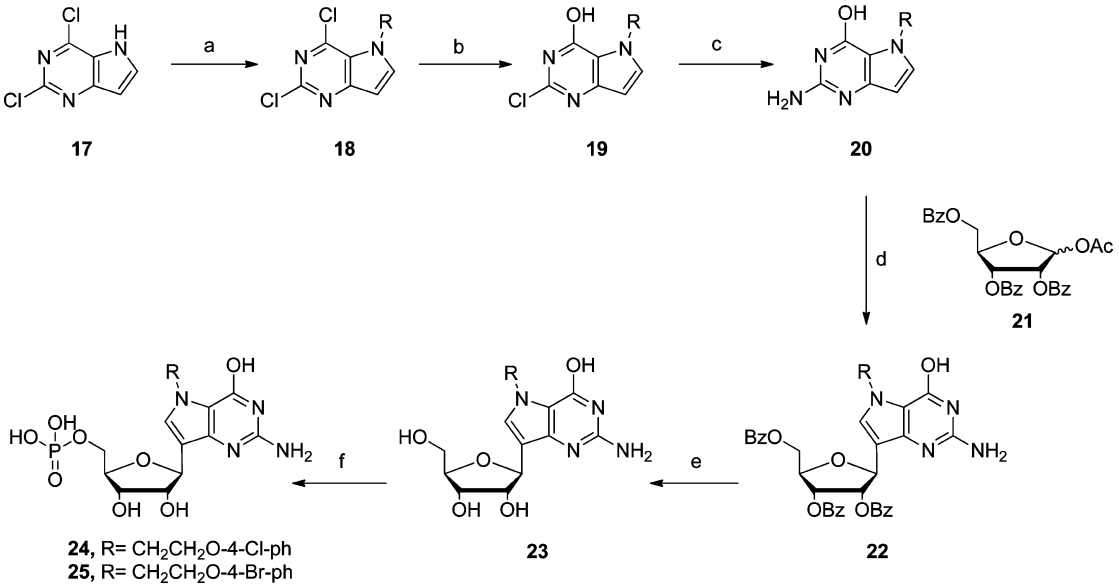

[a]Conditions: (a) NaH, 4-Cl-PhOCH$_2$CH$_2$Br (for **24**) or 4-BrPhOCH$_2$CH$_2$Br (for **25**), MeCN, 55°C; (b) aq 1 M NaOH, 1,4-dioxane, reflux; (c) 7 N NH$_3$ in MeOH, 170 °C; (d) $SnCl_4$, β-D-ribofuranose 1-acetate 2,3,5-tribenzoate, $MeNO_2$, 60°C; (e) NaOMe, MeOH, 23°C; (f) $POCl_3$, $PO(MeO)_3$; 0 °C.

Table 2. eIF4E Binding Affinity Comparison of N7-Modified Guanosine 5-Monophosphate *vs* N9-Modified Deazaguanine 5-Monophosphate Analogues

Structure	X	Compound	SPA IC_{50} (μM)
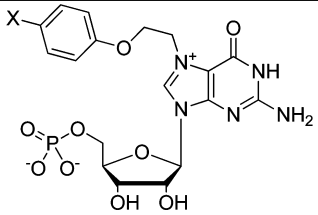	Cl	**9**	0.059±0.02 (n=4)
	Br	**10**	0.041±0.02 (n=3)
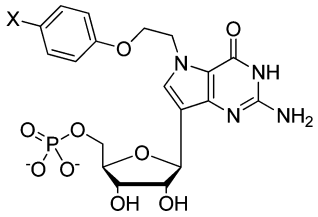	Cl	**24**	6.58±2.6(n=2)
	Br	**25**	3.6

compound **8**. More importantly, compounds **9**, **10**, and **12** were about 30-fold more effective inhibitors of cap dependent mRNA translation in a rabbit reticular lysate in vitro translation assay (RRL-IVT) than m7-GMP .

The cocrystal structure of eIF4E complexed with **9** was determined to a resolution of 2.7 Å. The structure revealed that **9** maintains the same binding mode as that of m7-GTP in the cap-binding slot with the *p*-chlorophenoxy ethyl group fitting pocket I almost perfectly, in both shape and size (Figure 2a). The chlorophenyl moiety makes numerous favorable van der Waals interactions with residues including Val153, Asp90, Phe48, Leu60, and Pro100 lining pocket I. The Cl atom is in close van der Waals contact with Phe48, Leu60, and Ser92, but there are no specific interactions with the oxygen atom of the phenoxyethyl linker. The rest of the molecule adopts a binding mode similar to that of m7-GTP (Figure 2b). Overall, there are no significant movements within the protein upon the binding of the Cl-phenoxy ethyl group. We noticed that the side chain of Ser92 adopts an alternative conformation to accommodate the binding of the Cl-atom. In addition, the side chains of Asp90, Trp56, and Met101 also shift to accommodate the phenyl group. The Glu103 side chain shows some shift as well but still maintains good H-bond interactions with the amino-guanosine moiety. Subsequent to our work, Brown et al. reported a similar effort on generating guanosine derivatives for targeting eIF4E activity.[29] While our GMP analogues target the pocket I behind Trp56 (Figure 2), both their 7-benzyl-GMP (Bn^{7}GMP) and 7-(*p*-fluorobenzyl)-GMP (Fbn^{7}GMP) com-

dx.doi.org/10.1021/jm300037x | J. Med. Chem. 2012, 55, 3837−3851

pounds make an induced fit to pocket III around Trp102 (Figure 1).

Apparently, the para-Cl atom prevents the phenyl ring from sampling other smaller pockets, further stabilizing the ligand binding. It was found that the chlorine atom can also be replaced by a bromo or a cyano group while retaining the binding potency. Disubstitution of the aryl ring was not tolerated. The chlorophenoxy ethyl group seems to fit the binding pocket very well. Simple replacement of the linker oxygen atom with a carbon atom resulted in a 100-fold loss of activity in the SPA assay. Thermodynamic analysis indicated that there is a 0.5 kcal/mol energy difference between the global energy minimum of compound **9** in water and its bound conformation.[30] However, for compound **7** there is a 3.0 kcal/mol difference between its global energy minimum in water and the bound conformation, indicating a larger penalty upon binding for this compound. This may explain the potency difference between compounds **7** and **9**.

The eIF4E binding potency relies to a significant extent on the delocalized positive charge of the guanine moiety, mainly due to favorable cation-π interactions with Trp56 and Trp102 and a decrease in overall negative molecular charge, which likely reduces the desolvation penalty upon binding. However, a highly charged molecule is generally incompatible with cell permeability. After establishing the ideal side chain at the N7 position, we moved on to investigate 9-deazaguanosine analogues to possibly eliminate the positive charge from the guanosine ring. The 9-deazaguanosine nucleoside was synthesized according to literature procedures shown in Scheme 2.[31] 2,4-Dichloro-5H-pyrrolo[3,2-d]pyrimidine **17** was alkylated with 1-(2-bromoethoxy)-4-chlorobenzene for compound **24** or 1-(2-bromoethoxy)-4-bromobenzene for compound **25** to yield ideal side-chain substituted pyrrolopyrimidine **18**. The dichloro group of 2,4-dichloropyrrolopyrimidin **18** was selectively hydrolyzed by treatment with NaOH to furnish compound **19**, which was then animated at the 2 position of **20**. The ribose moiety **21** was installed by a $SnCl_4$ catalyzed glycoside formation to give compound **22**. The benzoyl protecting groups of **22** were removed using NaOMe to give **23**, the 5-hydroxymethyl moiety of which was then phosphorylated to give compound **24**. Compound **25** was synthesized similarly.

It was found that the 9-deazaguanosine monophosphate **24** had 100-fold reduced binding affinity against eIF4E as compared to the 7-alkylated guanosine analogue **9** (Table 2). This was also true for the corresponding *p*-bromophenoxy ethyl derivatives **10** and **25**. The affinity differences between the 9-deazaguarnine and 7-methylguanine were consistent with those previously reported for GpppG compared with m7-GpppG, which was 276-fold weaker against eIF4E.[18] This SAR trend clearly indicated the importance of the positive charge for the formation of the cation-π interactions with Trp102 and Trp56. However, the 9-deazaguanosine monophosphates are still in the same affinity range as m7-GMP, validating our predictions that neutral analogues with appropriate features might be designed to replace the positively charged guanosine core.[25]

Next, we turned our attention toward designing analogues that would probe the role of the ribose moiety. The ribose ring is positioned at the entrance of the cap-binding site without participating in any specific interactions with the protein. Notably, the 2′- and 3′-hydroxyl groups of the ribose ring extend into a solvent accessible region. Indeed, we found that the incorporation of an isopropylidene group as in compound **26** (Table 3) had little or no effect on its binding affinity for eIF4E, consistent with previous observations.[21]

Table 3. eIF4E Binding Affinity Data for N7-Modified Guanosine 5-Monophosphate Analogues

Structure	Compound	SPA IC_{50} (μM)
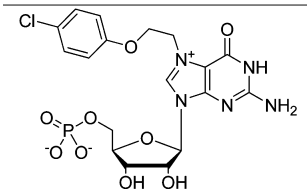	**9**	0.058±0.02(n=4)
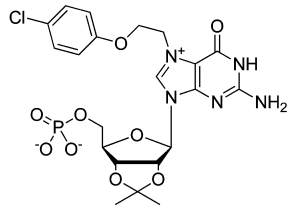	**26**	0.051

Inspection of the three-dimensional structure of the complex of **9** bound to eIF4E revealed that the ribose ring only provided a conformationally restricted connection linking the phosphate group with the guanine ring in a "folded-back" orientation. As previously noted, the two hydroxyl groups on the 3- and 4-positions of the ribose ring extend into the solvent accessible region without being engaged in any specific interaction with the eIF4E protein. The phosphate moiety on the 5′-position of the ribose was positioned approximately 4.2 Å away from the 8 position of the guanine (Figure 3). We reasoned that it should be possible to use an alternate linker extending from the 8-position of the guanine as a means of connecting the phosphate group with the guanine ring. Because deletion of the ribose would also decrease hydrophilicity, this modification might be anticipated to improve membrane permeability in those compounds. We sought to substitute the phosphate group with potential bioisosteric equivalents, such as a phosphonic acid or a carboxylic acid. Such groups would ideally be placed in the optimal position to interact with the residues Arg112, Arg157, and Lys162.

The designed compound **33** was synthesized as illustrated in Scheme 3. Since it had previously been found by us as well as others[24] that 2-methyl amine GMP analogues were about 2-fold more potent than 2-amino GMP analogues (data not shown), the final analogues were designed bearing a 2-methylamino group. The diamino compound **27** was synthesized via the published procedure.[32,33] The more basic amino group of the diamino compound **27** was first acetylated with 2-(4-chlorophenoxy)acetyl chloride to furnish compound **28**, which was subjected to borane reduction to generate the secondary amine **29**. The secondary amine **29** was then coupled with 4-bromobenzoic acid to furnish compound **30**. The ring closure was attempted with trimethylsilyl polyphosphanic acid treatment. However, the reaction only gave 20% yield of cyclization product **31**. We found that the ring closure can be accomplished more efficiently by treatment with *t*-BuONa to give **31** in 52% yield. . Palladium mediated reaction of **31** smoothly transferred the bromo group of **31** to a diethyl phosphonate **32**. The removal of one or both ethyl groups of

dx.doi.org/10.1021/jm300037x | J. Med. Chem. 2012, 55, 3837−3851

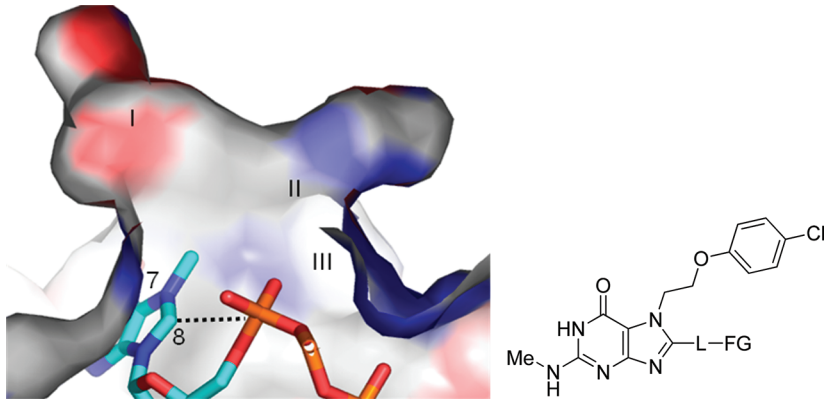

Figure 3. (a) Distance of phosphate group in relation to the 8 position of guanine in compound **9** bound to eIF4E; (b) possible design of 8-substituted N7-(chlorophenoxyethyl)guanine analogues. L: linker. FG: COOH, $PO(OH)_2$, SO_2NH_2, etc.

32 was accomplished by stirring the material with TMSBr in CH_2Cl_2 to yield final products **33** and **34**.

We determined the binding mode of compound **33** with an X-ray cocrystal structure at a resolution of 2.9 Å. This revealed that **33** adopts a binding mode similar to that of **9** (Figure 4a). While preserving the same H-bond interactions to the backbone amide of Trp120 and to the side chains of Glu103, the plane of the guanosine core is skewed about 10° in comparison with that of compound **9** (Figure 4b). The Cl-phenyl side-chain still occupies the binding pocket I very well, forming numerous favorable van der Waals interactions with the protein. The 8-phenyl moiety occupies the space between the guanosine and α-phosphate of the m7-GTP positions, which is less solvent exposed when compared to the ribose ring. Similar to the ribose, the phenyl group makes no specific interactions with eIF4E. The phosphonic acid moiety is positioned between the α- and β- phosphate groups of m7-GTP and forms direct H-bond interactions with Arg157 and Lys162. Due to the limitation of the diffraction resolution, very few water molecules were observed in the cocrystal structure. Thus, the water mediated H-bonds with Arg112 are not seen here. Overall, there are no significant conformational changes in the protein except for a slight shift of the side chain of Glu103, whose movement seems to be in concert with the guanosine ring rotation.

With the discovery of the phosphonic acid compound **33**, we carried out more detailed SAR studies of its analogues. The homologated phosphonic acid **39** was prepared starting from compound **35**.[34] The more basic amine was alkylated with 2-(4-chlorophenoxy)acetaldehyde through a reductive amination reaction to give compound **36**, which was then coupled with diethyl 4-(chlorocarbonyl)benzylphosphonate to generate compound **37**. The ring closure was achieved by heating compound **37** at reflux in 40% NaOMe in MeOH. The phosphonate ester was partially hydrolyzed to monomethyl ester **38** during the reaction. Deesterification was completed by treatment with TMSBr to furnish compound **39**. The difluoro substituted phosphonic acid **42** was similarly generated after acylation with 4-((diethoxyphosphoryl)difluoromethyl)benzoic acid[35] to give compound **40**. The carboxylic acid analogue **46** was generated by the same reaction sequence using methyl 4-(chlorocarbonyl)benzoate.

On the basis of the structural observation that the phosphonic acid moiety of compound **33** is situated between the α- and β-phosphates of m7-GTP, we envisioned that extending the phosphonic acid out by one carbon should be tolerated. Indeed, compound **39** was found to have similar affinity to compound **33**. Furthermore, the difluoro analogue **42** was 4-fold more active than the phosphonic acid **33**. While it is possible that the fluoro atoms are picking up additional hydrogen bonding interactions, it is more likely that these atoms simply increase the acidity of the phosphonic acid, thus strengthening its salt bridge interaction with Arg157 and Lys162. Discouragingly, the less charged carboxylic acid analogue **46** showed much reduced activity when compared with compound **33**.

Compound **33** is remarkably selective for eIF4E, with no significant off-target activities found at concentrations up to 10 μM in Upstate kinase panel and CEREP receptor panel screens. Unfortunately, however, compound **33** had compromised cell permeability with a P_{aap} of 1.1×10^{-6} cm/s (Table 4) in the PAMPA assay.[36] This is very likely due to the large polar surface area (PSA) contributed by the phosphonic acid moiety (calculated PSA for **33**: 142 $Å^2$) and its dianionic nature at physiological pH. This was confirmed by the diethyl phosphonate analogue **32**, which was significantly more permeable. Among the analogues, only the monoethyl phosphonate **34** and the carboxylic acid analogue **46** showed some affinity for eIF4E, as measured in the SPA assay (1.4 and 3.14 μM, respectively). Just like the mono phosphonic acid analogue **34**, the carboxylic acid analogue **46** showed limited cellular permeability.

CONCLUSION

In summary, we designed and synthesized a novel series of high affinity and selective eIF4E inhibitors starting from m7-GMP. Attaching a 4-phenylphosphonic acid moiety to the 8-position of the guanine ring gave a potent eIF4E inhibitor eliminating the ribose moiety, phosphate group, and positive charge. The presence of the ribose moiety was shown to be unnecessary for maintaining high levels of inhibitory activity. The biochemical activity of compound **33** is 95 nM for eIF4E in an SPA binding assay. More importantly, the compound has an IC_{50} of 2.5 μM for inhibiting cap-dependent mRNA translation in a rabbit reticular cell extract assay (RRL-IVT). Unfortunately, the compound displayed limited cellular permeability hindering its further evaluation in cellular assays. Further optimization or the potential use of prodrug strategies might be useful in increasing the cellular permeability of this series to achieve cellular activity and enable future testing *in vivo*. This series of potent, truncated analogues could serve as a promising new starting

Scheme 3. Synthesis of 8-Substituted N7-(Chlorophenoxyethyl) Guanine Analogues[a]

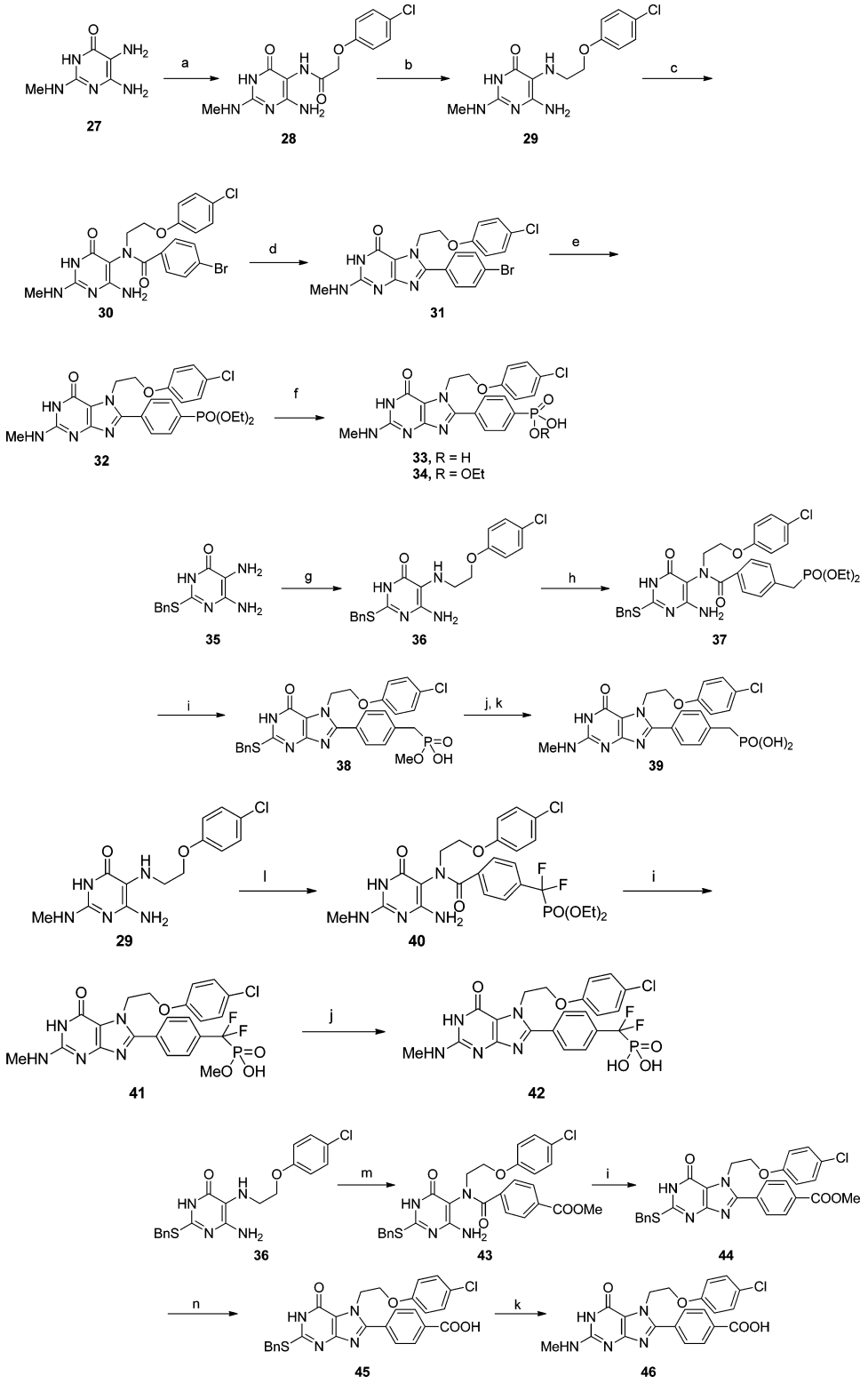

[a]Conditions: (a) 2-(4-chlorophenoxy)acetyl chloride, K_2CO_3, CH_2Cl_2, 66% yield; (b) BH_3, THF, 47% yield; (c) 4-bromobenzoic acid, HOBT, DMAP, EDC, DMF, 80% yield; (d) *t*-BuONa in *i*-PrOH, reflux, 52% yield; (e) $Pd(OAc)_2$, dicyclohexylmethylamine, diethyl phosphonate, 91% yield; (f) TMSBr, CH_2Cl_2, 42% yield for **33** and 92% yield for **34**; (g) $NaBH(OAc)_3$, 2-(4-chlorophenoxy)acetaldehyde, CH_2Cl_2, 32% yield; (h) Hunig's base, DMAP, diethyl 4-(chlorocarbonyl)benzylphosphonate, CH_2Cl_2; (i) 40% NaOMe/MeOH, 90° C, 15−66% yield; (j) TMSBr, DMF, 4.5% yield; (k) 40% $MeNH_2$, 160 °C, microwave, 25−68% yield; (l) Et_3N, HATU, 4-((diethoxyphosphoryl)difluoromethyl)benzoic acid; (m) Hunig's base, DMAP, methyl 4-(chlorocarbonyl)benzoate; (n) LiOH, MeOH, 100 °C, 74% yield.

dx.doi.org/10.1021/jm300037x | *J. Med. Chem.* 2012, 55, 3837−3851

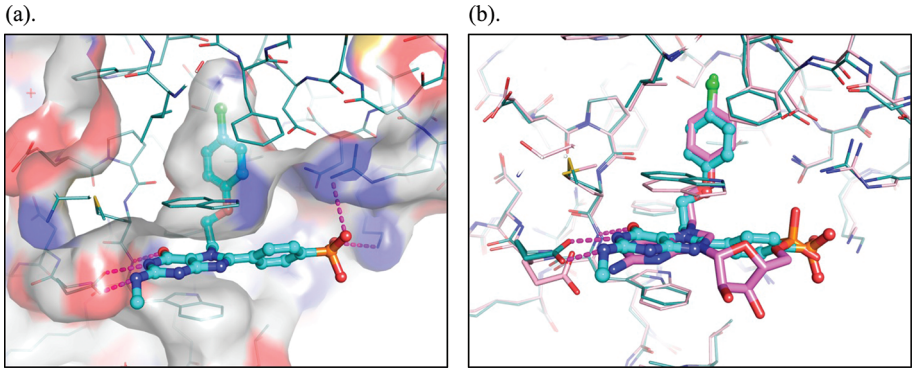

Figure 4. Binding of phosphonic acid analogue **33** in eIF4E. (a) Compound **33** in the cap-binding site of eIF4E. The protein is shown in molecular surface representation with selected residues involved in ligand recognition shown as sticks. The color scheme is the same as that in Figure 1 except that carbon atoms are colored in cyan. (b) Overlay of the cocrystal structures of compound **33** (in cyan) and **9** (in magenta) with eIF4E.

Table 4. eIF4E Binding Affinity Data for 8-Substituted N7-(Chlorophenoxyethyl) Guanine Analogues

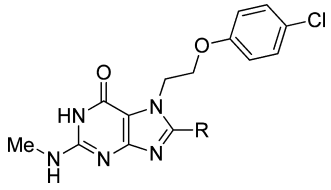

	R =	SPA IC50 (μM)	LLC-PK1 Paap (10^{-6}cm/s)
33	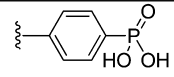	0.095±0.004 (n=2)	1.1
39	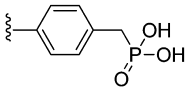	0.16±0.08 (n=2)	0.6
42	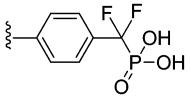	0.016±0.005 (n=2)	0.7
32	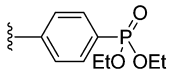	300	12.1
34	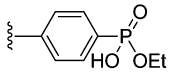	1.35	1.0
46	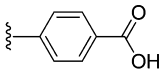	3.14±2.06 (n=3)	1.15

point toward the design of neutral eIF4E inhibitors with physicochemical properties suitable for cellular activity.

EXPERIMENTAL SECTION

General Experimental. Reagents and solvents used below were obtained from commercial sources and when required were purified. ^{1}H NMR spectra were obtained on a Varian Gemini 400 or 500 MHz NMR spectrometer. Electron ionization (EI) mass spectra were recorded on a Hewlett-Packard 5989A mass spectrometer. Electrospray ionization (ESI) mass spectrometry analysis was performed using a Hewlett-Packard 1100 MSD electrospray mass spectrometer using the HP1 100 HPLC for sample delivery. Combustion analyses were performed by Atlantic Microlab Inc. (Norcross, GA). Air and/or moisture sensitive reactions were carried out under N_2 using flame-dried glassware and standard syringe/septa techniques. HPLC method A: Analytical Agilent Eclipse Plus C_{18} 5 μm column, 4.6 mm × 150 mm, gradient elution of 10% MeCN in water to 100% MeCN in water over a 12 min period, where the CH_3CN and water contains 0.1% TFA. HPLC method B: Analytical Chromolith SpeedRod RP_{18} column (Merck, Darmstadt, Germany), 4.6 mm × 150 mm, gradient elution of 0% MeCN in water to 20% MeCN in water over a 4 min period, where the CH_3CN and water contains 0.1% TFA. HPLC method C: CAPCELL PAK C18, 4.6 mm × 75 mm, 3 μm column (Shiseido, Tokyo, Japan), gradient elution of 0% MeCN in water to 50% MeCN in water over a 4 min period, where the CH_3CN and water contains 0.1% TFA. HPLC method D: Analytical Agilent Eclipse Plus C_{18} 5 μm column, 4.6 mm × 150 mm, gradient elution of 10% MeCN in water to 100% MeCN in water over a 7.5 min period, where the CH_3CN and water contains 0.1% TFA. HPLC method E: CAPCELL PAK C18, 4.6 mm × 75 mm, 3 μm column (Shiseido, Tokyo, Japan), gradient elution of 0% MeCN in water to 100% MeCN in water over a 15 min period, where the CH_3CN and water contains 0.1% TFA. HPLC method F: Agilent SB-C8 column, gradient elution of 0% MeCN in water to 50% MeCN in water over a 1 min period, where the CH_3CN and water contains 0.1% TFA.

Synthetic Procedures and Characterization for Compounds. *7-(Benzyl)guanosine-5′-monophosphate (**2**).* To a slurry of guanosine-5′-monophosphate disodium salt hydrate (401 mg, 0.98 mmol, 1 equiv) in DMSO (5 mL) was added benzyl bromide (600 μL, 4.94 mmol, 5 equiv). The resulting white slurry was stirred at room temperature for 27 h; during this time, all solids dissolved. The reaction mixture was purified directly by reverse phase prep HPLC (Prep C_{18} OBD 10 μm column (Waters, Milford, MA), gradient elution of pure water to 15% MeCN in water over a 30 min period, where both solvents contain 0.1% TFA). After discarding mixed fractions, 61 mg (11%, 0.11 mmol) of the trifluoroactetate salt of **2** was isolated as a white solid: ^{1}H NMR (400 MHz, DMSO-d_6): δ 9.85 (s, 1 H), 7.52−7.58 (m, 2 H), 7.31−7.44 (m, 3 H), 5.85 (d, J = 3.3 Hz, 1 H), 5.58 (s, 2 H), 4.42−4.48 (m, 1 H), 4.11−4.23 (m, 3 H), 3.95−4.03 (m, 1 H); MS (LRES in negative mode) calcd for $C_{17}H_{19}N_5O_8P$ $[M - H]^-$ 452.1, found 452.0; HPLC method A t_R = 3.25 min, purity 98%.

*7-(3-Chlorobenzyl)guanosine-5′-monophosphate (**3**).* To a slurry of guanosine-5′-monophosphate disodium salt hydrate (302 mg, 0.74 mmol, 1 equiv) in DMSO (3.6 mL) was added 3-chlorobenzyl bromide (350 μL, 2.59 mmol, 3.5 equiv). The resulting white slurry was stirred at room temperature for 22 h; during this time all solids dissolved. The reaction mixture was purified directly by reverse phase prep HPLC (Prep C_{18} OBD 10 μm column (Waters, Milford, MA), gradient elution of 5% MeCN in water to 30% MeCN in water over a 30 min period, where both solvents contain 0.1% TFA). After discarding mixed fractions, 61 mg (14%, 0.10 mmol) of the trifluoroactetate salt of **3** was isolated as a white solid: ^{1}H NMR (400 MHz, DMSO-d_6): δ 9.70 (s, 1 H), 7.62 (s, 1 H), 7.46−7.51 (m, 1 H), 7.39−7.44 (m, 2 H), 5.85 (d, J = 3.1 Hz, 1 H), 5.57 (s, 2 H),

dx.doi.org/10.1021/jm300037x | J. Med. Chem. 2012, 55, 3837−3851

4.43−4.49 (m, 1 H), 4.12−4.23 (m, 3 H), 3.98−4.07 (m, 1 H); MS (LRES in negative mode) calcd for $C_{17}H_{18}ClN_5O_8P$ $[M - H]^-$ 486.1, found 486.1; HRMS: theoretical 490.0889, observed 490.0886; HPLC method A t_R = 4.13 min, purity 98%.

*7-(2-Chlorobenzyl)guanosine-5′-monophosphate (**4**).* To a slurry of guanosine-5′-monophosphate disodium salt hydrate (521 mg, 1280 μmol, 1 equiv) in DMSO (6 mL) was added 2-chlorobenzyl bromide (498 μL, 3839 μmol, 3 equiv). The resulting white slurry was stirred at room temperature for 2 days; during this time all solids dissolved. The reaction mixture was filtered and purified directly by reverse phase prep HPLC (Prep C_{18} OBD 10 μm column (Waters, Milford, MA), gradient elution of 0 to 30% MeCN in water over a 30 min period, where both solvents contain 0.1% TFA). After discarding mixed fractions, 110 mg (18%, 0.23 mmol) of the trifluoroacetate salt of **4** was isolated as a white solid: ^{1}H NMR (400 MHz, DMSO-d_6) δ ppm 9.65 (s, 1 H), 7.52 (dd, J = 8.0, 1.37 Hz, 1 H), 7.38 (dt, J = 7.6, 1.96 Hz, 1 H), 7.31 (dt, J = 7.6, 1.17 Hz, 1 H), 7.22 (dd, J = 7.8, 1.56 Hz, 1 H), 5.89 (d, J = 3.1 Hz, 1 H), 5.70 (s, 2 H), 4.49−4.58 (m, 1 H), 4.21 (t, J = 5.1 Hz, 1 H), 4.09−4.18 (m, 2 H), 3.92−4.05 (m, 1 H); MS (LRES in negative mode) calcd for $C_{17}H_{18}ClN_5O_8P$ $[M - H]^-$ 486.1, found 486.1; HRMS: theoretical 490.0889, observed 490.0892, HPLC method B t_R = 2.11 min, purity 100%.

*7-(4-Chlorobenzyl)guanosine-5′-monophosphate (**5**).* To a slurry of guanosine-5′-monophosphate disodium salt hydrate (250 mg, 0.61 mmol, 1 equiv) in DMSO (3.1 mL) was added 4-chlorobenzyl bromide (625 mg, 2.95 mmol, 4.8 equiv). The resulting white slurry was stirred at room temperature for 22 h; during this time all solids dissolved. The reaction mixture was purified directly by reverse phase prep HPLC (Prep C_{18} OBD 10 μm column (Waters, Milford, MA), gradient elution of 2% MeCN in water to 20% MeCN in water over a 30 min period, where both solvents contain 0.1% TFA). After discarding mixed fractions, 139 mg (38%, 0.23 mmol) of the trifluoroacetate salt of **5** was isolated as a white solid: ^{1}H NMR (400 MHz, DMSO-d_6): δ 9.94 (s, 1 H), 7.58 (d, J = 8.4 Hz, 2 H), 7.39 (d, J = 8.6 Hz, 2 H), 5.84 (d, J = 3.1 Hz, 1 H), 5.57 (s, 2 H), 4.41−4.47 (m, 1 H), 4.10−4.24 (m, 3 H), 3.93−4.01 (m, 1 H); MS (LRES in negative mode) calcd for $C_{17}H_{18}ClN_5O_8P$ $[M - H]^-$ 486.1, found 486.1; HRMS: theoretical 490.0889, observed 490.0893; HPLC method A, t_R = 4.21 min, purity 97%.

*7-(4-Chlorophenethyl)guanosine-5′-monophosphate (**6**).* To a slurry of guanosine-5′-monophosphate disodium salt hydrate (299 mg, 0.73 mmol, 1 equiv) in DMSO (4.5 mL) was added 4-chlorophenethyl bromide (550 μL, 3.67 mmol, 5.0 equiv). The resulting white slurry was heated at 50 °C for 26 h; during this time all solids dissolved. The reaction mixture was purified directly by reverse phase prep HPLC (Prep C_{18} OBD 10 μm column (Waters, Milford, MA), gradient elution of 5% MeCN in water to 30% MeCN in water over a 30 min period, where both solvents contain 0.1% TFA). Heavily mixed fractions were discarded, and the remaining impure product was purified again by reverse phase prep HPLC (Prep C_{18} OBD 10 μm column (Waters, Milford, MA), gradient elution of 10% MeCN in water to 25% MeCN in water over a 30 min period, where both solvents contain 0.1% TFA). After discarding mixed fractions, 3.2 mg (1%, 0.005 mmol) of the trifluoroacetate salt of **6** was isolated as a white solid: ^{1}H NMR (400 MHz, DMSO-d_6): δ 9.94 (s, 1 H), 7.58 (d, J = 8.4 Hz, 2 H), 7.39 (d, J = 8.6 Hz, 2 H), 5.84 (d, J = 3.1 Hz, 1 H), 5.57 (s, 2 H), 4.41−4.47 (m, 1 H), 4.10−4.24 (m, 3 H), 3.93−4.01 (m, 1 H); MS (LRES in negative mode) calcd for $C_{17}H_{18}ClN_5O_8P$ $[M - H]^-$ 486.1, found 486.1; HPLC method A, t_R = 4.43 min, purity 90%.

*7-(4-(Chlorophenyl)propyl)guanosine-5′-monophosphate (**7**).* The compound was prepared according to the same procedure used in preparing compound **2**. Purification by reverse-phase preparative HPLC (SB C8, 30 mm × 250 mm, 5 μm column; Agilent, Santa Clara, CA) (eluent: 0.1% TFA in acetonitrile/water, gradient 2% to 30% over 25 min) to provide the trifluoroacetate salt of **7** as a white solid (79.3 mg, 13% yield). ^{1}H NMR (400 MHz, DMSO-d_6) δ ppm 9.56 (1 H, s), 7.24−7.28 (2 H, m), 7.17−7.22 (2 H, m), 5.81 (1 H, d, J = 3.1 Hz), 4.36−4.44 (3 H, m), 4.11−4.22 (3 H, m), 3.99 (1 H, m), 2.61− 2.68 (2 H, m), 2.18−2.22 (2 H, m); MS (ESI) 514.2 $[M - 2H]^-$; HRMS: theoretical 516.1046, observed 516.1052; HPLC method C, t_R = 3.09 min, purity 98%.

*7-(Phenoxyethyl)guanosine-5′-monophosphate (**8**).* To a slurry of guanosine-5′-monophosphate disodium salt hydrate (500 mg, 1.20 mmol, 1 equiv) in DMSO (12 mL) was added phenyl-2-bromoethyl ether (1.20 g, 6.0 mmol, 5 equiv). The resulting white slurry was stirred at room temperature for 3 days and then heated to 50 °C for an additional 21 h; during the heating period, all solids dissolved. A portion of the reaction mixture was purified directly by reverse phase prep HPLC (Prep C_{18} OBD 10 μm column (Waters, Milford, MA), gradient elution of 2% MeCN in water to 20% MeCN in water over a 30 min period, where both solvents contain 0.1% TFA). After discarding mixed fractions, 3.2 mg (0.4%, 0.005 mmol) of the trifluoroacetate salt of **8** was isolated as a white solid: ^{1}H NMR (400 MHz, DMSO-d_6): δ 9.55 (s, 1 H), 7.23−7.31 (m, 2 H), 6.88−6.96 (m, 3 H), 5.89 (d, J = 3.9 Hz, 1 H), 5.70−5.79 (m, 1 H), 4.73−4.81 (m, 2 H), 4.44−4.51 (m, 1 H), 4.42 (t, J = 5.3 Hz, 2 H), 4.13−4.21 (m, 3 H), 3.99−4.07 (m, 2 H); MS (LRES in negative mode) calcd for $C_{18}H_{21}N_5O_9P$ $[M - H]^-$ 482.1, found 482.0; HRMS: theoretical 486.1384, observed 486.1387; HPLC method A, t_R = 3.96 min, purity 93%.

*7-(4-Chlorophenoxyethyl)guanosine-5′-monophosphate (**9**).* To a slurry of guanosine-5′-monophosphate disodium salt hydrate (380 mg, 0.93 mmol, 1 equiv) in DMSO (4.3 mL) was added 4-chlorophenyl-2-bromoethyl ether (879 mg, 3.73 mmol, 4 equiv). The resulting white slurry was heated 55 °C for 3.5 days; during this time all solids dissolved. The reaction mixture was purified directly by reverse phase prep HPLC (Prep C_{18} OBD 10 μm column (Waters, Milford, MA), gradient elution of 10% MeCN in water to 30% MeCN in water over a 30 min period, where both solvents contain 0.1% TFA). After discarding mixed fractions, 23.1 mg (4%, 0.037 mmol) of the trifluoroacetate salt of **9** was isolated as a white solid: ^{1}H NMR (400 MHz, DMSO-d_6): δ 9.65 (s, 1 H), 7.47 (br s, 1 H), 7.26 (d, J = 8.6 Hz, 2 H), 6.93 (d, J = 9.0 Hz, 2 H), 5.86 (d, J = 3.9 Hz, 1 H), 4.77 (br s, 2 H), 4.47 (t, J = 3.9 Hz, 1 H), 4.40 (t, J = 5.1 Hz, 2 H), 4.20 (t, J = 4.7 Hz, 1 H), 4.09−4.18 (m, 2 H), 3.95−4.05 (m, 2 H); ^{13}C NMR (125 MHz, DMSO-d_6): δ 157.2, 156.5, 154.1, 150.0, 137.4, 129.9, 125.5, 117.0, 107.6, 89.9, 84.5, 74.7, 70.1, 66.1, 64.5, 48.8; MS (HRES in negative mode) calcd for $C_{18}H_{20}ClN_5O_9P$ $[M - H]^-$ 516.1, found 516.1. HRMS: theoretical 516.0693, observed 516.0695; HPLC method A, t_R = 3.88 min, purity 95%.

*7-(4-Bromophenoxyethyl)guanosine-5′-monophosphate (**10**).* To a slurry of guanosine-5′-monophosphate disodium salt hydrate (329 mg, 0.81 mmol, 1 equiv) in DMSO (4.3 mL) was added 4-bromophenyl-2-bromoethyl ether (816 mg, 2.91 mmol, 3.6 equiv). The resulting white slurry was heated 55 °C for 4.5 days; during this time all solids dissolved. The reaction mixture was purified directly by reverse phase prep HPLC (Prep C_{18} OBD 10 μm column (Waters, Milford, MA), gradient elution of 10% MeCN in water to 30% MeCN in water over a 30 min period, where both solvents contain 0.1% TFA). After discarding mixed fractions, 13.7 mg (2.5%, 0.02 mmol) of the trifluoroacetate salt of **10** was isolated as a white solid: ^{1}H NMR (400 MHz, DMSO-d_6): δ 9.76 (s, 1 H), 7.42 (d, J = 8.8 Hz, 2 H), 6.92 (d, J = 8.9 Hz, 2 H), 5.87 (d, J = 3.7 Hz, 1 H), 4.74−4.82 (m, 2 H), 4.48 (t, J = 4.1 Hz, 1 H), 4.38−4.45 (m, 2 H), 4.20 (t, J = 4.6 Hz, 1 H), 4.09−4.17 (m, 2 H), 3.93−4.04 (m, 2 H); MS (LRES in negative mode) calcd for $C_{18}H_{20}BrN_5O_9P$ $[M - H]^-$ 560.0, found 560.0; HRMS: theoretical 562.0333, observed 562.0323; HPLC method A, t_R = 4.64 min, purity 96%.

*7-(4-Fluorophenoxyethyl)guanosine-5′-monophosphate (**11**).* To a slurry of guanosine-5′-monophosphate disodium salt hydrate (331 mg, 0.813 mmol, 1 equiv) in DMSO (4.3 mL) was added 1-(2-bromoethoxy)-4-fluorobenzene (641 mg, 2.93 mmol, 3.6 equiv). The resulting white slurry was heated at 55 °C for 3 days; during this time all solids dissolved and the reaction turned yellow. The reaction mixture was purified directly by reverse phase prep HPLC (Prep C_{18} OBD 10 μm column (Waters, Milford, MA), gradient elution of 10 to 30% MeCN in water over a 30 min period, where both solvents contain 0.1% TFA). Heavily mixed fractions were discarded, and the remaining impure product was purified again by reverse phase prep

HPLC (Prep C_{18} OBD 10 μm column (Waters, Milford, MA), gradient elution of 2% MeCN in water to 20% MeCN in water over a 30 min period, where both solvents contain 0.1% TFA). After discarding mixed fractions, 2 mg (0.4%, 0.003 mmol) of the trifluoroactetate salt of **11** was isolated as a white solid: ^{1}H NMR (400 MHz, DMSO-d_6) δ ppm 9.79 (s, 1 H), 7.00−7.14 (m, 2 H), 6.89−6.99 (m, 2 H), 5.86 (d, J = 3.9 Hz, 1 H), 4.77 (t, J = 5.09 Hz, 2 H), 4.46−4.51 (m, 1 H), 4.40 (t, J = 5.3 Hz, 2 H), 4.19−4.27 (m, 1 H), 4.13 (d, J = 2.74 Hz, 2 H), 3.97 (d, J = 5.9 Hz, 1 H); MS (LRES in negative mode) calcd for $C_{18}H_{21}FN_5O_9P$ $[M - H]^-$ 500.1, found 500.0; HRMS: theoretical 502.1134, observed 502.1132, HPLC method A, t_R = 7.52 min, purity 96%.

*7-(4-Cyanophenoxyethyl)guanosine-5′-monophosphate (**12**).* To a slurry of guanosine-5′-monophosphate disodium salt hydrate (0.53 g, 1.3 mmol, 1 equiv) in DMSO (4.5 mL) was added 4-(2-bromoethoxy)benzonitrile (0.88 g, 3.9 mmol, 3 equiv). The resulting white slurry was stirred at 60 °C for 28 h; during this time all solids dissolved. The reaction mixture was filtered and purified directly by reverse phase prep HPLC (Prep C_{18} OBD 10 μm column (Waters, Milford, MA), gradient elution of 10−30% MeCN in water over a 30 min period, where both solvents contain 0.1% TFA). The lyophilized impure product was suspended in water and then fully dissolved by adding 2 equiv of 1 N NaOH to pH = 8. The solution was then acidified to pH = 4 by adding 1 equiv of 1 N HCl. The solution was extracted with EtOAc and *n*-butanol to remove impurities, and then it was lyophilzed to afford **12** was as a white solid: ^{1}H NMR (400 MHz, DMSO-d_6) δ ppm 10.11 (s, 1 H), 7.70 (d, J = 8.6 Hz, 2 H), 7.12 (d, J = 8.6 Hz, 2 H), 5.84 (d, J = 3.5 Hz, 1 H), 4.83 (s, 2 H), 4.53 (dt, J = 13.7, 4.11 Hz, 3 H), 4.28 (t, J = 4.3 Hz, 1 H), 4.09 (s, 2 H), 3.89 (br. s, 1 H); MS (LRES in negative mode) calcd for $C_{19}H_{20}N_6O_9P$ $[M - H]^-$ 507.1, found 507.1; HRMS: theoretical 509.1180, observed 502.1179, HPLC method A, t_R= 4.33 min, purity 100%.

*7-(4-Trifluoromethylphenoxyethyl)guanosine-5′-monophosphate (**13**).* To a slurry of guanosine-5′-monophosphate disodium salt hydrate (0.53 g, 1.3 mmol, 1 equiv) in DMSO (4.5 mL) was added 1-(2-bromoethoxy)-4-(trifluoromethyl)benzene (1.1 g, 3.9 mmol, 3 equiv). The resulting white slurry was stirred at 55 °C for 3 days; during this time all solids dissolved. The reaction mixture was purified directly by reverse phase prep HPLC (Prep C_{18} OBD 10 μm column (Waters, Milford, MA), gradient elution of 10 to 30% MeCN in water over a 30 min period, where both solvents contain 0.1% TFA). After discarding mixed fractions, 2 mg (0.02%, 0.03 mmol) of the trifluoroactetate salt of **13** was isolated as a white solid: ^{1}H NMR (400 MHz, DMSO-d_6) δ ppm 9.79 (s, 1 H), 7.61 (d, J = 9.0 Hz, 2 H), 7.12 (d, J = 8.2 Hz, 2 H), 5.86 (d, J = 3.5 Hz, 1 H), 4.82 (t, J = 4.7 Hz, 2 H), 4.45−4.62 (m, 3 H), 4.23 (t, J = 4.7 Hz, 1 H), 4.14 (s, 2 H), 3.93−4.03 (m, 1 H); MS (LRES in positive mode) calcd for $C_{19}H_{21}F_3N_5O_9P$ $[M + H]^+$ 552.1, found 552.2; HPLC method D, t_R = 2.52 min, purity 81%.

*7-(3-Fluoro-4-Chlorophenoxyethyl)guanosine-5′-monophosphate (**14**).* To a slurry of guanosine-5′-monophosphate disodium salt hydrate (527 mg, 1.29 mmol, 1 equiv) in DMSO (4.5 mL) was added 4-(2-bromoethoxy)-1-chloro-2-fluorobenzene (1.3 g, 5.2 mmol, 4 equiv). The resulting white slurry was stirred at 55 °C for 4 days; during this time all solids dissolved and starting material still remained. The reaction mixture was filtered and purified directly by reverse phase prep HPLC (Prep C_{18} OBD 10 μm column (Waters, Milford, MA), gradient elution of 10 to 30% MeCN in water over a 30 min period, where both solvents contain 0.1% TFA). After discarding mixed fractions, 12 mg (1.7%, 0.02 mmol) of the trifluoroactetate salt of **14** was isolated as a white solid: ^{1}H NMR (400 MHz, DMSO-d_6) δ ppm 9.70 (s, 1 H), 7.36 (t, J = 8.8 Hz, 2 H), 7.02 (dd, J = 11.4, 2.7 Hz, 1 H), 6.76 (ddd, J = 8.8, 2.7, 1.0 Hz, 1 H), 5.80 (d, J = 3.5 Hz, 1 H), 4.72 (t, J = 4.9 Hz, 2 H), 4.41−4.47 (m, 1 H), 4.34−4.41 (m, 2 H), 4.16 (t, J = 4.7 Hz, 1 H), 3.99−4.12 (m, 2 H), 3.87−3.94 (m, 1 H); MS (LRES in negative mode) calcd for $C_{18}H_{19}Cl\,FN_5O_9P$ $[M - H]^-$ 534.1, found 534.1; HRMS: theoretical 528.0682, observed 528.0675, HPLC method A, t_R = 6.71 min, purity 91%.

*7-(N-(4-Chlorophenyl)acetamido)guanosine-5′-monophosphate (**15**).* To a slurry of guanosine-5′-monophosphate disodium salt hydrate (551 mg, 1.35 mmol, 1 equiv) in DMSO (4.5 mL) was added 2-chloro-*N*-(4-chlorophenyl)acetamide (828 mg, 4.06 mmol). The resulting white slurry was stirred at 55 °C for 2 days; during this time most of the solids dissolved. The reaction mixture was filtered and purified directly by reverse phase prep HPLC (Prep C_{18} OBD 10 μm column (Waters, Milford, MA), gradient elution of 17 to 27% MeCN in water over a 30 min period, where both solvents contain 0.1% TFA). After discarding mixed fractions, 5 mg (0.7%, 0.008 mmol) of the trifluoroactetate salt of **15** was isolated as a white solid: ^{1}H NMR (400 MHz, DMSO-d_6) δ ppm 11.35 (s, 1 H), 9.99 (s, 1 H), 7.60 (d, J = 9.0 Hz, 2 H), 7.33 (d, J = 9.0 Hz, 2 H), 5.90 (d, J = 3.1 Hz, 1 H), 5.43 (d, J = 16.0 Hz, 1 H), 5.33 (d, J = 16.4 Hz, 1 H), 4.38−4.52 (m, 1 H), 4.20−4.27 (m, 1 H), 4.09−4.18 (m, 2 H), 3.91 (dd, J = 9.6, 4.9 Hz, 1 H); MS (LRES in positive mode) calcd for $C_{18}H_{20}ClN_6O_9P$ $[M + H]^+$ 531.1, found 531.0; HPLC method A, t_R = 6.06 min, purity 85%.

*7-N-(5-Chloro-2-methylbenzofuranyl)guanosine-5′-monophosphate (**16**).* The compound was prepared according to the same procedure used in preparing compound **2**. Purification by reverse-phase preparative HPLC (SB C8, 30 mm × 250 mm, 5 μm column; Agilent, Santa Clara, CA) (eluent: 0.1% TFA in acetonitrile/water, gradient 5% to 40% over 25 min) to provide 44 mg (6.4%) of the trifluoroactetate salt of **16** as a white solid: ^{1}H NMR (500 MHz, DMSO-d_6) δ ppm 3.93−4.00 (m, 1 H), 4.11−4.15 (m, 1 H), 4.15−4.21 (m, 1 H), 4.26 (t, J = 5.3 Hz, 1 H), 4.47 (t, J = 3.7 Hz, 1 H), 5.78−5.92 (m, 3 H), 7.08 (s, 1 H), 7.31 (dd, J = 8.9, 2.1 Hz, 1 H), 7.57 (d, J = 8.9 Hz, 1 H), 7.67 (d, J = 1.8 Hz, 1 H), 9.95 (s, 1 H); MS (LRES in negative mode), found 526.0 $[M - 2H]^-$; HPLC method E, t_R = 11.3 min, purity 95%.

*2,4-Dichloro-5-(2-(4-chlorophenoxy)ethyl)-5H-pyrrolo[3,2-d]pyrimidine (**18**).* Sodium hydride (60% in mineral oil) (0.28 mL, 6.7 mmol) was added to an acetonitrile solution (75 mL) containing 2,4-dichloro-5H-pyrrolo[3,2-*d*]pyrimidine (1.000 g, 5.3 mmol). After stirring for 20 min at room temperature, 4-chlorophenyl 2-bromoethyl ether (1.5 g, 6.4 mmol) was added, and the resulting mixture was stirred overnight at 55 °C. The solution was then concentrated and purified on silica, eluting with 10−100% hexane/ethyl acetate gradient to give 1.7 g (94% yield) of 2,4-dichloro-5-(2-(4-chlorophenoxy)-ethyl)-5H-pyrrolo[3,2-*d*]pyrimidine. LCMS-ESI (POS), m/z, M + 1: Found 342, Calculated 342.

*2-Chloro-5-(2-(4-chlorophenoxy)ethyl)-5H-pyrrolo[3,2-d]pyrimidin-4-ol (**19**).* Aqueous 1 M sodium hydroxide (6 mL, 6 mmol) was added to a dioxane solution (60 mL) containing 2,4-dichloro-5-(2-(4-chlorophenoxy)ethyl)-5H-pyrrolo[3,2-*d*]pyrimidine (2.13 g, 6 mmol). The resulting mixture was stirred at reflux for 3 h and then cooled to room temperature and neutralized with acetic acid. After the mixture was cooled on ice, a precipitate formed and was collected (1.98 g, 99% yield). This material was used in the next step without further purification. LCMS-ESI (NEG), m/z, M − 1: Found 322, Calculated 322.

*2-Amino-5-(2-(4-chlorophenoxy)ethyl)-5H-pyrrolo[3,2-d]pyrimidin-4-ol (**20**).* 2-Chloro-5-(2-(4-chlorophenoxy)ethyl)-5H-pyrrolo[3,2-*d*]pyrimidin-4-ol (2 g, 6 mmol) was suspended in a methanolic ammonia solution (7 N, 50 mL), sealed in a Parr steel reactor, and heated at 170 °C overnight. The reaction was cooled to room temperature and purified on silica gel, eluting with a dichloromethane/methanol gradient (0−20%). Similar fractions were pooled and concentrated to give 1.56 g (84% yield) of 2-amino-5-(2-(4-chlorophenoxy)ethyl)-5H-pyrrolo[3,2-*d*]pyrimidin-4-ol: LCMS-ESI (POS), m/z, M + 1: Found 305, Calculated 305.

*(2S,3S,4R,5R)-2-(2-Amino-5-(2-(4-chlorophenoxy)ethyl)-4-hydroxy-5H-pyrrolo[3,2-d]pyrimidin-7-yl)-5-(benzoyloxymethyl)-tetrahydrofuran-3,4-diyl Dibenzoate (**22**).* Tin(IV) chloride (0.19 mL, 1.6 mmol) was added to a nitromethane (20 mL) solution containing β-D-ribofuranose 1-acetate 2,3,5-tribenzoate (0.35 g, 0.69 mmol) and 2-amino-5-(2-(4-chlorophenoxy)ethyl)-5H-pyrrolo[3,2-*d*]pyrimidin-4-ol (0.18 g, 0.58 mmol). The resulting mixture was stirred for 3 h at 60 °C. Excess solvent was then removed using reduced pressure, and the remaining residue was purified on silica, eluting with a dichloromethane/methanol gradient (0−20%), giving

0.11 g (26% yield) of pure product: LCMS-ESI (POS), *m/z*, M + 1: Found 749, Calculated 749.

*(2S,3R,4S,5R)-2-(5-(2-(4-Chlorophenoxy)ethyl)-4-hydroxy-2-(methylamino)-5H-pyrrolo[3,2-d]pyrimidin-7-yl)-5-(hydroxymethyl)tetrahydro-3,4-furandiol (**23**).* Sodium methoxide (0.081 g, 1.5 mmol) was added to a methanol solution (10 mL) containing (2*S*,3*S*,4*R*,5*R*)-2-(2-amino-5-(2-(4-chlorophenoxy)ethyl)-4-hydroxy-5H-pyrrolo[3,2-*d*]pyrimidin-7-yl)-5-(benzoyloxymethyl)-tetrahydrofuran-3,4-diyl dibenzoate (0.11 g, 0.15 mmol). The resulting mixture was stirred overnight at room temperature and then purified by reverse phase HPLC (5−70% water/acetonitrile gradient with 0.1% TFA). Desired fractions were pooled and lyophilized to give 40 mg (61% yield) of (2*S*,3*R*,4*S*,5*R*)-2-(2-amino-5-(2-(4-chlorophenoxy)-ethyl)-4-hydroxy-5H-pyrrolo[3,2-*d*]pyrimidin-7-yl)-5-(hydroxymethyl)tetrahydrofuran-3,4-diol: LCMS-ESI (POS), *m/z*, M + 1: Found 437, Calculated 437.

*((2R,3S,4R,5S)-5-(5-(2-(4-Chlorophenoxy)ethyl)-4-hydroxy-2-amino-5H-pyrrolo[3,2-d]pyrimidin-7-yl)-3,4-dihydroxytetrahydro-2-furanyl)methyl Dihydrogen Phosphate (**24**).* Phosphorus oxychloride (29 μL, 309 μmol) and trimethylphosphate (12 μL, 103 μmol) were premixed at 0 °C for 10 min and then added to (2*S*,3*R*,4*S*,5*R*)-2-(2-amino-5-(2-(4-chlorophenoxy)ethyl)-4-hydroxy-5H-pyrrolo[3,2-*d*]-pyrimidin-7-yl)-5-(hydroxymethyl)tetrahydrofuran-3,4-diol (0.045 g, 103 μmol). The mixture was stirred for 4 h and then diluted with water and purified directly via preparative HPLC (5−50% water/acetonitrile gradient with 0.1% TFA). Similar fractions were pooled and lyophilized, yielding 12 mg (23% yield) of final product: ^{1}H NMR (500 MHz, DMSO-d_6) δ ppm 3.81 −3.89 (m, 1 H), 3.89−4.06 (m, 4 H), 4.28 (t, *J* = 5.49 Hz, 2 H), 4.56−4.64 (m, 2 H), 4.66 (d, *J* = 7.32 Hz, 1 H), 6.96 (d, *J* = 9.16 Hz, 2 H), 7.31 (d, *J* = 9.16 Hz, 2 H), 7.42 (s, 1 H), 7.69−7.97 (m, 2 H). LCMS-ESI (POS), *m/z*, M + 1: Found 517, Calculated 517.

*((3aS,4S,6S,6aS)-6-(2-amino-7-(2-(4-chlorophenoxy)ethyl)-6-oxo-1H-purin-7-ium-9(6H)-yl)-2,2-dimethyltetrahydrofuro[3,4-d][1,3]-dioxol-4-yl)methyl Phosphate (**26**).* The 2′,3′-*O*-isopropylidieneguanosine (Sigma-Aldrich) (400 mg, 1.24 μmol) and 4-chlorophenyl 2-bromoethyl ether (Sigma-Aldrich) (874 mg, 3712 μmol) were dissolved in 3 mL of DMSO and heated at 60° for 3 days. The reaction was diluted in ethyl acetate and extracted three times with water. The product-containing aqueous layer was lyophilized to a clear yellowish oil which contained DMSO and product. Purification of the residue by preparatory RP-HPLC (10−30% acetonitrile, water, 0.1% TFA, gradient elution) over 30 min using a SunfireTM Prep C18 OBD column, 10 μm, 30 mm × 150 mm (Waters, Milford, MA) at 30 mL/min provided the alkylated product as a white solid after lyophilization to give 2-amino-7-(2-(4-chlorophenoxy)ethyl)-9-((3a*R*,4*R*,6*R*,6a*R*)-6-(hydroxymethyl)-2,2-dimethyltetrahydrofuro[3,4-*d*][1,3]dioxol-4-yl)-6-oxo-6,9-dihydro-1H-purin-7-ium (156 mg, 26%). LCMS, MS (neg ion) 477 [M − H]-Placed trimethyl phosphate (1.0 mL, 8686 μmol) at 0°, then $POCl_3$ was added (100 μL, 1085 μmol), followed by the 2-amino-7-(2-(4-chlorophenoxy)ethyl)-9-((3a*R*,4*R*,6*R*,6a*R*)-6-(hydroxy-methyl)-2,2-dimethyltetrahydrofuro[3,4-*d*][1,3]dioxol-4-yl)-6-oxo-6,9-dihydro-1H-purin-7-ium (52 mg, 109 μmol). Then the reaction was warmed to room temperature and stirred for 30 min. It was recooled to 0° and quenched with a small amount of $NaHCO_3$ (saturated) until pH ∼ 7. Purification of the solution by preparatory RP-HPLC (10 to 40% acetonitrile, water, 0.1% TFA, gradient elution) over 30 min using SunfireTM Prep C18 OBD column, 10 μm, 30 mm × 150 mm (Waters, Milford, MA) at 30 mL/min provided the phosphate product (31 mg, 49%) as a fluffy white powder after lyophilization. ^{1}H NMR (500 MHz, DMSO-d_6) δ ppm 1.33 (s, 3 H), 1.52 (s, 3 H), 3.97 (dt, *J* = 11.55, 5.84 Hz, 1 H), 4.05−4.20 (m, 1 H), 4.43 (dq, *J* = 11.62, 5.67 Hz, 2 H), 4.52 (br s, 1 H), 4.77 (br s, 2 H), 5.11 (dd, *J* = 6.11, 2.45 Hz, 1 H), 5.32 (d, *J* = 6.36 Hz, 1 H), 6.20 (s, 1 H), 6.99 (m, *J* = 8.80 Hz, 2 H), 7.32 (m, *J* = 8.80 Hz, 2 H), 9.45 (s, 1 H). LCMS, MS (neg ion) [M − 2H]$^-$ $C_{21}H_{24}ClN_5O_9P$ calc 556.1, found 556.1, HRMS: theoretical 558.1157, observed 558.1157, HPLC method A, t_R = 5.06 min, purity 99%.

*N-(4-Amino-2-(methylamino)-6-oxo-1,6-dihydropyrimidin-5-yl)-2-(4-chlorophenoxy)acetamide (**28**).* To 5,6-diamino-2-(methylamino)pyrimidin-4(3H)-one (44.15 g, 285 mmol) in a 1 L flask equipped with a mechanical stirrer was added potassium carbonate (34.3 g, 569 mmol). To this solution was added 4-chlorophenoxyacetyl chloride (44.4 mL, 285 mmol), dropwise and with stirring. The reaction needed occasional cooling in an ice bath to avoid overheating. When LCMS analysis indicated complete reaction, 400 mL of water was added. The resulting precipitate was filtered off. The solid was thoroughly washed with water and dried under reduced pressure to give 51.5 g of the first batch of compound. The aqueous layer was filtered again and washed with water to give 9.25 g of a second batch of material. The solid was vacuum-dried to give *N*-(4-amino-2-(methylamino)-6-oxo-1,6-dihydropyrimidin-5-yl)-2-(4-chlorophenoxy)acetamide (60.4 g, 65.6% yield).

*6-Amino-5-(2-(4-chlorophenoxy)ethylamino)-2-(methylamino)-pyrimidin-4(3H)-one (**29**).* A 1 M solution of BH_3·THF in THF (77 mL, 77 mmol) was added to a THF (100 mL) solution containing *N*-(4-amino-2-(methylamino)-6-oxo-1,6-dihydropyrimidin-5-yl)-2-(4-chlorophenoxy)acetamide (6.20 g, 19 mmol). The resulting mixture was stirred for 5 min at 23 °C and then at reflux for 1 h, at which point LCMS indicated the reaction was completed. To the reaction mixture was added methanol (5 mL) and 4 M HCL in dioxane (∼5 mL) slowly. A white precipitate formed. The suspension was heated for 10 h at reflux and then cooled to room temperature and concentrated. THF was then added to the solid, and the suspension was filtered to give the 6-amino-5-(2-(4-chlorophenoxy)ethylamino)-2-(methylamino)pyrimidin-4(3H)-one (3.5 g, 54% yield).

*N-(4-Amino-2-(methylamino)-6-oxo-1,6-dihydropyrimidin-5-yl)-4-bromo-N-(2-(4-chlorophenoxy)ethyl)benzamide (**30**).* To a solution of *p*-bromobenzoic acid (0.358 g, 1.78 mmol) in DMF (18 mL) was added HATU (1.02 g, 2.67 mmol) and *N*,*N*-diisopropylethylamine (1.24 mL, 7.12 mmol). The reaction mixture was stirred for half an hour before 6-amino-5-(2-(4-chlorophenoxy)ethylamino)-2-(methylamino)pyrimidin-4(3H)-one (0.607 g, 1.96 mmol) was added to the mixture. The combined reaction mixture was stirred at room temperature overnight. It was purified on silica gel, eluting with a dichloromethane/methanol gradient (0−20%). Similar fractions were pooled and concentrated to give *N*-(4-amino-2-(methylamino)-6-oxo-1,6-dihydropyrimidin-5-yl)-4-bromo-*N*-(2-(4-chlorophenoxy)ethyl)-benzamide (0.666 g, 75.9% yield).

*8-(4-Bromophenyl)-7-(2-(4-chlorophenoxy)ethyl)-2-(methylamino)-1H-purin-6(7H)-one (**31**).* To a solution of *N*-(4-amino-2-(methylamino)-6-oxo-1,6-dihydropyrimidin-5-yl)-4-bromo-*N*-(2-(4-chlorophenoxy)ethyl)benzamide (0.666 g, 1.35 mmol) in iPrOH (10 mL) dried over molecular sieves was added sodium *tert*-butoxide (0.649 g, 6.76 mmol). The reaction mixture was stirred at 100 °C overnight. Next the reaction mixture was acidified with acetic acid (0.34 mL, 5.9 mmol) and concentrated to give 8-(4-bromophenyl)-7-(2-(4-chlorophenoxy)ethyl)-2-(methylamino)-1H-purin-6(7H)-one (0.334 g, 52.1% yield).

*Diethyl 4-(7-(2-(4-Chlorophenoxy)ethyl)-6-hydroxy-2-(methylamino)-7H-purin-8-yl)phenylphosphonate (**32**).* To the starting material in a 25 mL sealed tube was added EtOH, palladium(II) acetate (0.95 mg, 4.2 μmol), diethyl phosphite (6.5 μL, 51 μmol), and *N*,*N*-dicyclohexylmethylamine (13 μL, 63 μmol) under Ar. The mixture was purged with Ar for 10 min, and triphenyl phosphine (2.0 μL, 8.4 μmol) was added. The reaction mixture was stirred at 100 °C overnight. The solvent was removed under vacuum. The crude product was purified by chromatoraphy on silica gel, eluting with 0−10% MeOH−CH_2Cl_2 to give diethyl 4-(7-(2-(4-chlorophenoxy)-ethyl)-6-hydroxy-2-(methylamino)-7H-purin-8-yl)phenylphosphonate (17 mg, 76% yield). ^{1}H NMR (500 MHz, chloroform-*d*) δ ppm 1.37 (t, *J* = 7.09 Hz, 6 H), 2.97 (br s, 3 H), 4.02−4.26 (m, 4 H), 4.43 (t, *J* = 5.01 Hz, 2 H), 4.72 (t, *J* = 5.01 Hz, 2 H), 6.56−6.78 (m, 2 H), 7.06−7.23 (m, 2 H), 7.83−8.07 (m, 5 H).

*Ethyl Hydrogen (4-(7-(2-(4-Chlorophenoxy)ethyl)-6-hydroxy-2-(methylamino)-7H-purin-8-yl)phenyl)phosphonate (**34**).* To diethyl 4-(7-(2-(4-chlorophenoxy)ethyl)-6-hydroxy-2-(methylamino)-7H-purin-8-yl)phenylphosphonate (20 mg, 37.6 μmol) in a 10 mL flask was added CH_2Cl_2 and bromotrimethylsilane (30 μL, 224 μmol). The solution was stirred at 30 °C over 24 h. The solvent was removed under vacuum, and the residue was purified by reverse phase HPLC to

give ethyl hydrogen (4-(7-(2-(4-chlorophenoxy)ethyl)-6-hydroxy-2-(methylamino)-7H-purin-8-yl)phenyl)phosphonate (8.0 mg, 42% yield). ^{1}H NMR (500 MHz, DMSO-d_6) δ ppm 1.31 (t, J = 8.0 Hz, 3 H), 2.81 (d, J = 4.65 Hz, 3 H), 4.31 (t, J = 5.26 Hz, 2 H), 4.51 (q, J = 8.0 Hz, 2 H), 4.63 (t, J = 5.14 Hz, 2 H), 6.06 (d, J = 4.65 Hz, 1 H), 6.77 (m, J = 9.05 Hz, 2 H), 7.25 (m, J = 8.80 Hz, 2 H), 7.79−8.03 (m, 4 H), 10.90 (s, 1 H). HRMS: theoretical 472.1387, observed 472.1385; HPLC method F, t_R = 0.657 min, purity 97%.

*4-(7-(2-(4-Chlorophenoxy)ethyl)-6-hydroxy-2-(methylamino)-7H-purin-8-yl)phenylphosphonic Acid (**33**).* To diethyl 4-(7-(2-(4-chlorophenoxy)ethyl)-6-hydroxy-2-(methylamino)-7H-purin-8-yl)-phenylphosphonate (17 mg, 32 μmol) in a 10 mL flask was added CH_2Cl_2 and bromotrimethylsilane (30 μL, 224 μmol). The solution was stirred at 30 °C over 3 days. The solvent was removed under vacuum, and the residue was purified by reverse phase HPLC to give 4-(7-(2-(4-chlorophenoxy)ethyl)-6-hydroxy-2-(methylamino)-7H-purin-8-yl)phenylphosphonic acid (14 mg, 92% yield). ^{1}H NMR (500 MHz, DMSO-d_6) δ ppm 2.81 (d, J = 4.65 Hz, 3 H), 4.31 (t, J = 5.26 Hz, 2 H), 4.63 (t, J = 5.14 Hz, 2 H), 6.06 (d, J = 4.65 Hz, 1 H), 6.77 (m, J = 9.05 Hz, 2 H), 7.25 (m, J = 8.80 Hz, 2 H), 7.79−8.03 (m, 4 H), 10.90 (s, 1 H). HRMS: theoretical 444.1074, observed 444.1073; HPLC method F, Agilent SB-C8 column, 10−50% H_2O−CH_3CN, t_R = 0.457 min, purity 98%.

*6-Amino-2-(benzylthio)-5-(2-(4-chlorophenoxy)ethylamino)-pyrimidin-4(3H)-one (**36**).* 5,6-Diamino-2-(benzylthio)pyrimidin-4(3H)-one (7.09 g, 28.6 mmol) and 2-(4-chlorophenoxy)acetaldehyde (4.87 g, 28.5 mmol) were combined with methylene chloride (80.00 mL, 1225 mmol) and stirred at room temperature for 60 min. The reaction was cooled to room temperature. Next, sodium triacetoxyborohydride (18.18 g, 85.8 mmol) was added. The reaction was stirred at room temperature overnight. The reaction was quenched with water. The reaction was diluted with dichloromethane and water until all solids were dissolved. The aqueous layer was extracted with dichloromethane three times. The organics were combined and washed with brine. The chloromethane layer was filtered through Na_2SO_4 and concentrated in vacuum. The crude material was purified on silica gel eluting with a dichloromethane/methanol gradient (0−20%) to give 6-amino-2-(benzylthio)-5-(2-(4-chlorophenoxy)-ethylamino)pyrimidin-4(3H)-one (3.72 g, 32.3% yield).

*Diethyl 4-((4-Amino-2-(benzylthio)-6-oxo-1,6-dihydropyrimidin-5-yl)(2-(4-chlorophenoxy)ethyl)carbamoyl)benzylphosphonate (**37**).* Triethyl phosphite (6.07 mL, 35.4 mmol) was added to a toluene solution containing p-(bromomethyl)benzoic acid (6.92 g, 32.2 mmol). The resulting mixture was stirred overnight at 111 °C. The solvent was then removed using reduced pressure, and the remaining residue was used in the next step without purification. LCMS-ESI (NEG), m/z, M − 1: Found 271, Calculated 271.

DMF (5 drops) was added to a DCM solution containing oxalyl chloride (0.305 mL, 3.44 mmol) and 4-((diethoxyphosphoryl)-methyl)benzoic acid (0.468 g, 1.72 mmol). The resulting mixture was stirred for 3 h at room temperature. The mixture was then concentrated and used in the next step without purification.

Hunig's base (0.300 mL, 1.72 mmol) and dimethylaminopyridine (0.210 g, 1.72 mmol) were added to a DCM (40 mL) solution containing 6-amino-2-(benzylthio)-5-(2-(4-chlorophenoxy)-ethylamino)pyrimidin-4(3H)-one (0.693 g, 1.72 mmol) and diethyl 4-(chlorocarbonyl)benzylphosphonate (0.500 g, 1.72 mmol) . The resulting mixture was stirred overnight at 23 °C. The solution was then washed with water, dried over sodium sulfate, and concentrated. This material was used in the next step without further purification. LCMS-ESI (POS), m/z, M + 1: Found 657, Calculated 657.

*Methyl Hydrogen 4-(2-(Benzylthio)-7-(2-(4-chlorophenoxy)ethyl)-6-oxo-6,7-dihydro-1H-purin-8-yl)benzylphosphonate (**38**).* Diethyl 4-((4-amino-2-(benzylthio)-6-oxo-1,6-dihydropyrimidin-5-yl)(2-(4-chlorophenoxy)ethyl)carbamoyl)benzylphosphonate (0.170 g, 0.259 mmol) was suspended in 6 mL of a 40% NaOMe/MeOH solution and heated to 90 °C for 1 h. After cooling to room temperature, concentrated HCl was added until the solution was acidic. Excess solvent was then removed, and the remaining solid was washed repeatedly with absolute ethanol. The filtrate was concentrated, and the resulting residue was purified by reverse phase HPLC using a C-8 Agilent column, eluting with a 10−90% water/acetonitrile gradient with 0.1% TFA. Desired fractions were pooled and concentrated (0.101 g, 66% yield). LCMS-ESI (POS), m/z, M + H_2O: Found 615, Calculated 615.

*(4-(7-(2-(4-Chlorophenoxy)ethyl)-2-(methylamino)-6-oxo-6,7-dihydro-1H-purin-8-yl)benzyl)phosphonic Acid (**39**).* Bromotrimethylsilane (0.188 mL, 1.42 mmol) was added to a DMF solution containing methyl hydrogen 4-(2-(benzylthio)-7-(2-(4-chlorophenoxy)ethyl)-6-oxo-6,7-dihydro-1H-purin-8-yl)-benzylphosphonate (0.170 g, 0.285 mmol). The resulting mixture was stirred overnight at room temperature. Next, a few drops of methanol were added, and the resulting mixture was purified directly by reverse phase HPLC using a C-8 Agilent column, eluting with a 10−90% water/acetonitrile gradient with 0.1% TFA. Desired fractions were pooled and lyophilized to give 0.143 g (86% yield) of pure product. LCMS-ESI (POS), m/z, M + 1: Found 583, Calculated 583.

An aqueous 40% methyl amine solution (2 mL) containing 4-(2-(benzylthio)-7-(2-(4-chlorophenoxy)ethyl)-6-oxo-6,7-dihydro-1H-purin-8-yl)benzylphosphonic acid (5 mg, 9 umol) was sealed in a tube and heated in a microwave at 160 °C for 12 h. The reaction was then concentrated to dryness, and the resulting residue was purified by reverse phase HPLC using a C-8 Agilent column, eluting with a 5−50% water/acetonitrile gradient with 0.1% TFA. Desired fractions were pooled and lyophilized to give 3 mg (68% yield) of pure product. ^{1}H NMR (400 MHz, MeOH) δ ppm 2.86 (s, 3 H), 4.34 (t, J = 4.99 Hz, 2 H), 4.65−4.72 (m, 2 H), 6.58−6.70 (m, 2 H), 7.01−7.15 (m, 2 H), 7.49 (d, J = 6.46 Hz, 2 H), 7.69 (d, J = 8.02 Hz, 2 H); LCMS-ESI (POS), m/z, M + 1: Found 490, Calculated 490. HPLC method F, 20−95% H_2O−CH_3CN, t_R = 0.227 min, purity: 97%.

*Methyl Hydrogen ((4-(7-(2-(4-Chlorophenoxy)ethyl)-2-(methylamino)-6-oxo-6,7-dihydro-1H-purin-8-yl)phenyl)difluoromethyl)-phosphonate (**41**).* Diethyl bromodifluoromethylphosphonate (0.877 mL, 4.94 mmol) was added to a dry DMF solution containing cadmium (0.0704 mL, 5.41 mmol) (under nitrogen). The resulting mixture was stirred at room temperature for 2 h and then filtered into a flask containing copper(I) chloride (0.097 mL, 3.46 mmol) and benzyl 4-iodobenzoate (1.00 g, 2.96 mmol) (under nitrogen). The resulting mixture was stirred overnight at room temperature. The reaction was then purified on silica, eluting with a hexane/ethyl acetate gradient (0−100%). Desired fractions were pooled and concentrated to give 1.06 g (90.8% yield) of pure product. LCMS-ESI (POS), m/z, M + 1: Found 399, Calculated 399.

10% palladium on carbon (0.290 g, 2.70 mmol) was added to an ethanol solution containing benzyl 4-((diethoxyphosphoryl)-difluoromethyl)benzoate (1.6 g, 2.68 mmol). The suspension was then placed under an atmosphere of hydrogen (1 atm) and stirred vigorously for 4 h. Next, the solution was filtered though Celite and concentrated. This material was used in the next step without further purification (0.83 g, 100% crude yield). LCMS-ESI (NEG), m/z, M − 1: Found 307, Calculated 307.

Triethylamine (0.045 mL, 0.32 mmol) was added to a DMF (100 mL) solution containing 4-((diethoxyphosphoryl)difluoromethyl)-benzoic acid (0.100 g, 0.32 mmol) and 6-amino-5-(2-(4-chlorophenoxy)ethylamino)-2-(methylamino)pyrimidin-4(3H)-one (0.20 g, 0.65 mmol). The resulting mixture was stirred for 6 h at 23 °C. The solution was then partitioned with water/ethyl acetate, and the organic layer was dried over sodium sulfate and concentrated. This material was then suspended in a 25% NaOMe/MeOH solution and was heated at 90 °C for 1 h. Next, concentrated HCl was added until the pH was 1 and the solvent was removed. The resulting solid was washed with absolute ethanol, and the filtrate was collected and concentrated. This material was used in the next step without further purification. LCMS-ESI (POS), m/z, M + 1: Found 540, Calculated 540.

*((4-(3-(2-(4-Chlorophenoxy)ethyl)-6-(methylamino)-4-oxo-4,5-dihydro-3H-imidazo[4,5-c]pyridin-2-yl)phenyl)difluoromethyl)-phosphonic Acid (**42**).* Bromotrimethylsilane (73 μL, 556 μmol) was added to a DMF (1 mL) solution containing methyl hydrogen (4-(7-(2-(4-chlorophenoxy)ethyl)-2-(methylamino)-6-oxo-6,7-dihydro-1H-

purin-8-yl)phenyl)difluoromethylphosphonate (30 mg, 56 μmol). The resulting mixture was stirred for 2 h at 60 °C. The mixture was then directly injected on reverse phase HPLC using a C-8 Agilent column eluting with a 5−50% water/acetonitrile gradient with 0.1% TFA. Desired fractions were pooled and lyophilized to give 1.3 mg (4.5% yield) of pure product. ^{1}H NMR (500 MHz, MeOH) δ ppm 2.99 (s, 3 H), 4.48 (t, *J* = 5.01 Hz, 2 H), 4.84 (t, *J* = 5.01 Hz, 2 H), 6.71−6.89 (m, 2 H), 7.16−7.29 (m, 2 H), 7.94 (s, 4 H). LCMS-ESI (POS), *m*/*z*, M + 1: Found 526, Calculated 526, Agilent SB-C8 column, 10−50% H_2O−CH_3CN, HPLC method F, t_R = 0.422 min, purity 100%.

*Methyl 4-(2-(Benzylthio)-7-(2-(4-chlorophenoxy)ethyl)-6-oxo-6,7-dihydro-1H-purin-8-yl)benzoate (**44**).* *N*,*N*-Dimethylpyridin-4-amine (0.121 g, 0.993 mmol) and *N*-ethyl-*N*-isopropylpropan-2-amine (0.128 g, 0.993 mmol) were added to a DCM (40 mL) solution containing 6-amino-2-(benzylthio)-5-(2-(4-chlorophenoxy)ethylamino)pyrimidin-4(3H)-one (0.400 g, 0.993 mmol) and methyl 4-(chlorocarbonyl)-benzoate (0.197 g, 0.993 mmol). The resulting mixture was stirred for 3 h at 23 °C. The solution was then partitioned with water, dried over sodium sulfate, and concentrated. The remaining residue was suspended in a 40% NaOMe/MeOH solution and was heated at 90 °C for 1 h. The reaction was then cooled to room temperature, and concentrated HCl was added until the pH was 1. Excess solvent was removed, and the resulting solid was washed with absolute ethanol. The filtrate was concentrated, and the remaining residue was purified on silica, eluting with DCM/MeOH stepwise gradient (0−20%). Desired fractions were pooled and concentrated (0.0831 g, 15% yield). LCMS-ESI (POS), *m*/*z*, M + 1: Found 547, Calculated 547.

*4-(2-(Benzylthio)-7-(2-(4-chlorophenoxy)ethyl)-6-oxo-6,7-dihydro-1H-purin-8-yl)benzoic Acid (**45**).* Lithium hydroxide (4 mg, 0.15 mmol) was added to a water/MeOH (1:1) (30 mL) solution containing methyl 4-(2-(benzylthio)-7-(2-(4-chlorophenoxy)ethyl)-6-oxo-6,7-dihydro-1H-purin-8-yl)benzoate (0.0831 g, 0.15 mmol). The resulting mixture was stirred for 2 h at 100 °C. The material was then acidified and concentrated. The residue was washed with absolute ethanol, and the filtrated was concentrated. This material was used in the next step without purification (0.60 g, 74% crude yield). LCMS-ESI (POS), *m*/*z*, M + 1: Found 533, Calculated 533.

*4-(7-(2-(4-Chlorophenoxy)ethyl)-2-(methylamino)-6-oxo-6,7-dihydro-1H-purin-8-yl)benzoic acid (**46**).* An aqueous methylamine 40% wt solution (2 mL) and 4-(2-(benzylthio)-7-(2-(4-chlorophenoxy)ethyl)-6-oxo-6,7-dihydro-1H-purin-8-yl)benzoic acid (0.025 g, 0.047 mmol) were sealed in a tube and heated in a microwave at 160 °C for 12 h. The reaction was then concentrated to dryness, and the resulting residue was purified by reverse phase HPLC using a C-8 Agilent column eluting with a 5−50% water/acetonitrile gradient with 0.1% TFA. The desired fractions were pooled and lyophilized to give 5.19 mg (25% yield) of pure product. ^{1}H NMR (400 MHz, MeOH) δ ppm 2.87 (s, 3 H), 4.33 (s, 2 H), 4.71 (s, 2 H), 6.62 (m, *J* = 9.00 Hz, 2 H), 7.06 (m, *J* = 9.19 Hz, 2 H), 7.83 (m, *J* = 8.41 Hz, 2 H), 8.11 (m, *J* = 8.41 Hz, 2 H); LCMS-ESI (POS), *m*/*z*, M + 1: Found 440, Calculated 440. Agilent SB-C8 column, 20−95% H_2O−CH_3CN, HPLC method F, t_R = 0.286 min, purity 100%.

Biological Characterization of Compounds. *Protein Production and Crystallography.* Recombinant eIF4E protein for crystallographic studies was prepared as previously reported.[20,37] In brief, the full length human eIF4E was cloned into vector pET101 with an N-terminal FLAG 6xHis tag followed by an rTEV cleavage site. The protein was expressed in *E. coli* and purified through a m7-GTP-sepharose column. The purified protein which contained 100 μM m7-GTP was then concentrated to about 7 mg/mL in 20 mM Hepes, pH 7.6, 100 mM KCl, 1 mM DTT, 0.1 mM EDTA for crystallization. The m7-GTP-bound eIF4e protein was crystallized by the hanging drop vapor diffusion method at 16 °C with a 1:1 ratio of protein solution to reservoir solution of 17−20% PEG-3350 and 0.1−0.4 M Na formate. The compound was introduced to the crystals by a soaking method in a solution of 32% PEG-3350, 0.4 M Na formate, 10% glycerol with powder compound. Harvested crystals were transferred to the mother liquor with 30% glycerol and then flash frozen in liquid nitrogen. The X-ray diffraction data sets were collected at the synchrotron beamlines 501/502 at Advanced Light Source (ALS) in Berkeley, and they were processed with the programs MOSFLM[38] and SCALA in the CCP4 program suite.[39] The structures were solved by the molecular replacement method MOLREP[40] using a previously published eIF4E structure (PDB code: 1IPB) as a search model. Model building and refinement were carried out in QUANTA (Accelrys, San Diego), COOT,[41] and REFMAC[42] in CCP4.[39] All structural figures were prepared using Pymol (http://www.pymol.org).

In Vitro IC_{50} Determination: SPA Assay. Human eIF4E protein (NP_001959) was produced as an N-terminal FLAG-6xHis fusion protein in *E. coli* and purified by m7-GTP-sepharose affinity chromatography (GE Healthcare). Protein was eluted with 100 μM m7-GDP and dialyzed extensively into storage buffer. For binding analysis, eIF4E protein (50 nM final) was biotinylated and bound to streptaviden coated scintillation proximity assay beads (GE Healthcare) in the presence of ^{3}H-m7-GTP (1 mCi/mL, Moravek Biochemicals) in binding buffer (20 mM HEPES, pH 7.4, 50 mM KCL, 1 mM DTT, and 0.5 mM EDTA). To determine competitive inhibition of eIF4E binding, compounds were added in an 11 point, 3-fold dilution dose series, and loss of the radioactive signal was monitored by scintillation counting. Assays were performed in triplicate, and IC_{50} values were calculated by nonlinear regression curve fitting using GraphPad Prism analysis software (GraphPad Software).

In Vitro IC_{50} Determination: Rabbit Reticulocyte Lysate In Vitro Translation Assay. Inhibition of cap dependent translation was measured in vitro by utilization of the pRenilla-HCV-Firefly (pRIF) luciferase reporter mRNA. The pRIF reporter construct was generated by insertion of renilla and firefly luciferase cDNAs into multiple cloning sites of the pIRES vector (Clonetech) using standard techniques. The HCV internal ribosome entry site (bases 14−383) was cloned into Mlu-1, Sal-1 restriction sites located between renilla and firefly cDNAs. For in vitro transcription, the pRIF plasmid was linearized by digestion with Bgl-II and m7-GTP capped, poly adenylated mRNA was transcribed with T7 polymerase according to manufacturer's guidelines (Ambion, AM1345). In vitro translations were performed in 20 μL reactions containing 5 μL of rabbit reticulocyte lysate (Promega), 100 mM potassium acetate, 1.4 mM magnesium chloride, 10 μM amino acids, 20 units of RNasin (Promega), and 20 ng of pRIF mRNA. eIF4E inhibitor compounds were added in an 11 point, 3-fold dilution dose series with a final DMSO concentration of 1%. Reactions were incubated at 30 °C for 90 min prior to determination of renilla and firefly luciferase activities (Promega, Dual-Glo E2920). Assays were performed in triplicate, and IC_{50} values were calculated by nonlinear regression curve fitting using GraphPad Prism analysis software (GraphPad Software).

■ ASSOCIATED CONTENT

Accession Codes

[†]Coordinates of the crystal structures have been deposited with the RCSB Protein Data Bank with the accession codes of 4DT6 and 4DUM.

■ AUTHOR INFORMATION

Corresponding Author

*Phone: (650) 244-2596 (X.C.) and (650) 244-2446 (Z.W.). E-mail: xiaoqic@amgen.com and zwang@amgen.com.

Notes

The authors declare no competing financial interest.

■ ACKNOWLEDGMENTS

We thank Larry McGee for critical reading of the manuscript. The Advanced Light Source is supported by the Director, Office of Science, Office of Basic Sciences, Materials Sciences Division, of the U.S. Department of Energy under Contract No.

DE-AC03-76SF00098 at the Lawrence Berkeley National Laboratory.

REFERENCES

(1) Hanahan, D.; Weinberg, R. A. The hallmarks of cancer. *Cell* **2000**, *100* (1), 57−70.

(2) Blagden, S. P.; Willis, A. E. The biological and therapeutic relevance of mRNA translation in cancer. *Nat. Rev. Clin. Oncol.* **2011**, *8* (5), 280−91.

(3) Silvera, D.; Formenti, S. C.; Schneider, R. J. Translational control in cancer. *Nat. Rev. Cancer* **2010**, *10* (4), 254−66.

(4) Mamane, Y.; Petroulakis, E.; Rong, L.; Yoshida, K.; Ler, L. W.; Sonenberg, N. eIF4E—from translation to transformation. *Oncogene* **2004**, *23* (18), 3172−9.

(5) Merrick, W. C. H.; John, W. B. *The Pathway and Mechanism of Eukaryotic Protein Synthesis*; Cold Spring Harbor Laboratory Press: Cold Spring Harbor, NY, 1996; Vol. *30*, pp 31−69.

(6) Kerekatte, V.; Smiley, K.; Hu, B.; Smith, A.; Gelder, F.; De Benedetti, A. The proto-oncogene/translation factor eIF4E: a survey of its expression in breast carcinomas. *Int. J. Cancer* **1995**, *64* (1), 27−31.

(7) Rosenwald, I. B.; Chen, J. J.; Wang, S.; Savas, L.; London, I. M.; Pullman, J. Upregulation of protein synthesis initiation factor eIF-4E is an early event during colon carcinogenesis. *Oncogene* **1999**, *18* (15), 2507−17.

(8) Nathan, C. O.; Liu, L.; Li, B. D.; Abreo, F. W.; Nandy, I.; De Benedetti, A. Detection of the proto-oncogene eIF4E in surgical margins may predict recurrence in head and neck cancer. *Oncogene* **1997**, *15* (5), 579−84.

(9) Wang, S.; Rosenwald, I. B.; Hutzler, M. J.; Pihan, G. A.; Savas, L.; Chen, J. J.; Woda, B. A. Expression of the eukaryotic translation initiation factors 4E and 2alpha in non-Hodgkin's lymphomas. *Am. J. Pathol.* **1999**, *155* (1), 247−55.

(10) Topisirovic, I.; Guzman, M. L.; McConnell, M. J.; Licht, J. D.; Culjkovic, B.; Neering, S. J.; Jordan, C. T.; Borden, K. L. Aberrant eukaryotic translation initiation factor 4E-dependent mRNA transport impedes hematopoietic differentiation and contributes to leukemogenesis. *Mol. Cell. Biol.* **2003**, *23* (24), 8992−9002.

(11) Iborra, F. J.; Jackson, D. A.; Cook, P. R. Coupled transcription and translation within nuclei of mammalian cells. *Science* **2001**, *293* (5532), 1139−42.

(12) Rousseau, D.; Kaspar, R.; Rosenwald, I.; Gehrke, L.; Sonenberg, N. Translation initiation of ornithine decarboxylase and nucleocytoplasmic transport of cyclin D1 mRNA are increased in cells overexpressing eukaryotic initiation factor 4E. *Proc. Natl. Acad. Sci. U.S.A.* **1996**, *93* (3), 1065−70.

(13) Cohen, N.; Sharma, M.; Kentsis, A.; Perez, J. M.; Strudwick, S.; Borden, K. L. PML RING suppresses oncogenic transformation by reducing the affinity of eIF4E for mRNA. *EMBO J.* **2001**, *20* (16), 4547−59.

(14) Topisirovic, I.; Culjkovic, B.; Cohen, N.; Perez, J. M.; Skrabanek, L.; Borden, K. L. The proline-rich homeodomain protein, PRH, is a tissue-specific inhibitor of eIF4E-dependent cyclin D1 mRNA transport and growth. *EMBO J.* **2003**, *22* (3), 689−703.

(15) Topisirovic, I.; Capili, A. D.; Borden, K. L. Gamma interferon and cadmium treatments modulate eukaryotic initiation factor 4E-dependent mRNA transport of cyclin D1 in a PML-dependent manner. *Mol. Cell. Biol.* **2002**, *22* (17), 6183−98.

(16) Bjornsti, M. A.; Houghton, P. J. Lost in translation: dysregulation of cap-dependent translation and cancer. *Cancer Cell* **2004**, *5* (6), 519−23.

(17) Avdulov, S.; Li, S.; Michalek, V.; Burrichter, D.; Peterson, M.; Perlman, D. M.; Manivel, J. C.; Sonenberg, N.; Yee, D.; Bitterman, P. B.; Polunovsky, V. A. Activation of translation complex eIF4F is essential for the genesis and maintenance of the malignant phenotype in human mammary epithelial cells. *Cancer Cell* **2004**, *5* (6), 553−63.

(18) Graff, J. R.; Konicek, B. W.; Vincent, T. M.; Lynch, R. L.; Monteith, D.; Weir, S. N.; Schwier, P.; Capen, A.; Goode, R. L.; Dowless, M. S.; Chen, Y.; Zhang, H.; Sissons, S.; Cox, K.; McNulty, A. M.; Parsons, S. H.; Wang, T.; Sams, L.; Geeganage, S.; Douglass, L. E.; Neubauer, B. L.; Dean, N. M.; Blanchard, K.; Shou, J.; Stancato, L. F.; Carter, J. H.; Marcusson, E. G. Therapeutic suppression of translation initiation factor eIF4E expression reduces tumor growth without toxicity. *J. Clin. Invest.* **2007**, *117* (9), 2638−48.

(19) Tomoo, K.; Matsushita, Y.; Fujisaki, H.; Abiko, F.; Shen, X.; Taniguchi, T.; Miyagawa, H.; Kitamura, K.; Miura, K.; Ishida, T. Structural basis for mRNA cap-binding regulation of eukaryotic initiation factor 4E by 4E-binding protein, studied by spectroscopic, X-ray crystal structural, and molecular dynamics simulation methods. *Biochim. Biophys. Acta* **2005**, *1753* (2), 191−208.

(20) Tomoo, K.; Shen, X.; Okabe, K.; Nozoe, Y.; Fukuhara, S.; Morino, S.; Ishida, T.; Taniguchi, T.; Hasegawa, H.; Terashima, A.; Sasaki, M.; Katsuya, Y.; Kitamura, K.; Miyoshi, H.; Ishikawa, M.; Miura, K. Crystal structures of 7-methylguanosine 5′-triphosphate (m(7)GTP)- and P(1)-7-methylguanosine-P(3)-adenosine-5′,5′-triphosphate (m(7)GpppA)-bound human full-length eukaryotic initiation factor 4E: biological importance of the C-terminal flexible region. *Biochem. J.* **2002**, *362* (Pt 3), 539−44.

(21) Niedzwiecka, A.; Marcotrigiano, J.; Stepinski, J.; Jankowska-Anyszka, M.; Wyslouch-Cieszynska, A.; Dadlez, M.; Gingras, A. C.; Mak, P.; Darzynkiewicz, E.; Sonenberg, N.; Burley, S. K.; Stolarski, R. Biophysical studies of eIF4E cap-binding protein: recognition of mRNA 5′ cap structure and synthetic fragments of eIF4G and 4E-BP1 proteins. *J. Mol. Biol.* **2002**, *319* (3), 615−35.

(22) Marcotrigiano, J.; Gingras, A. C.; Sonenberg, N.; Burley, S. K. Cap-dependent translation initiation in eukaryotes is regulated by a molecular mimic of eIF4G. *Mol. Cell* **1999**, *3* (6), 707−16.

(23) Marcotrigiano, J.; Gingras, A. C.; Sonenberg, N.; Burley, S. K. Cocrystal structure of the messenger RNA 5′ cap-binding protein (eIF4E) bound to 7-methyl-GDP. *Cell* **1997**, *89* (6), 951−61.

(24) Ghosh, P.; Chunkyung, P.; Peterson, M. S.; Bitterman, P. B.; Polunovsky, V. A.; Wagner, C. R. Synthesis and evaluation of potential inhibitors of eIF4E cap binding to 7-methyl GTP. *Bioorg. Med. Chem. Lett.* **2005**, *15* (8), 2177−2180.

(25) Cai, A.; Jankowska-Anyszka, M.; Centers, A.; Chlebicka, L.; Stepinski, J.; Stolarski, R.; Darzynkiewicz, E.; Rhoads, R. E. Quantitative assessment of mRNA cap analogues as inhibitors of in vitro translation. *Biochemistry* **1999**, *38* (26), 8538−47.

(26) Darzynkiewicz, E.; Stepinski, J.; Ekiel, I.; Goyer, C.; Sonenberg, N.; Temeriusz, A.; Jin, Y.; Sijuwade, T.; Haber, D.; Tahara, S. M. Inhibition of eukaryotic translation by nucleoside 5′-monophosphate analogues of mRNA 5′-cap: changes in N7 substituent affect analogue activity. *Biochemistry* **1989**, *28* (11), 4771−8.

(27) Ghosh, B.; Benyumov, A. O.; Ghosh, P.; Jia, Y.; Avdulov, S.; Dahlberg, P. S.; Peterson, M.; Smith, K.; Polunovsky, V. A.; Bitterman, P. B.; Wagner, C. R. Nontoxic chemical interdiction of the epithelial-to-mesenchymal transition by targeting cap-dependent translation. *ACS Chem. Biol.* **2009**, *4* (5), 367−77.

(28) Giri, R. S.; Thaker, H. M.; Giordano, T.; Chen, B.; Nuthalapaty, S.; Vasu, K. K.; Sudarsanam, V. Synthesis and evaluation of quinazolinone derivatives as inhibitors of NF-kappaB, AP-1 mediated transcription and eIF-4E mediated translational activation: inhibitors of multi-pathways involve in cancer. *Eur. J. Med. Chem.* **2010**, *45* (9), 3558−63.

(29) Brown, C. J.; McNae, I.; Fischer, P. M.; Walkinshaw, M. D. Crystallographic and mass spectrometric characterisation of eIF4E with N7-alkylated cap derivatives. *J. Mol. Biol.* **2007**, *372* (1), 7−15.

(30) Guimaraes, C. R.; Kopecky, D. J.; Mihalic, J.; Shen, S.; Jeffries, S.; Thibault, S. T.; Chen, X.; Walker, N.; Cardozo, M. Thermodynamic analysis of mRNA cap binding by the human initiation factor eIF4E via free energy perturbations. *J. Am. Chem. Soc.* **2009**, *131* (50), 18139−46.

(31) Girgis, N. S.; Michael, M. A.; Smee, D. F.; Alaghamandan, H. A.; Robins, R. K.; Cottam, H. B. Direct C-glycosylation of guanine analogues: the synthesis and antiviral activity of certain 7- and 9-deazaguanine C-nucleosides. *J. Med. Chem.* **1990**, *33* (10), 2750−5.

(32) Roth, B.; Smith, J. M., Jr.; Hultquist, M. E. Analogs of Pteroylglutamic Acid. VII. 2-Alkylamino Derivatives. *J. Am. Chem. Soc.* **1951**, *73*, 2864−2868.
(33) Matysiak, S.; Waldscheck, B.; Pfleiderer, W. Nucleosides. LXV. Synthesis of new pteridine-N8-nucleosides. *Nucleosides, Nucleotides Nucleic Acids* **2004**, *23* (1−2), 51−66.
(34) Loewe, R. S.; Ambroise, A.; Muthukumaran, K.; Padmaja, K.; Lysenko, A. B.; Mathur, G.; Li, Q.; Bocian, D. F.; Misra, V.; Lindsey, J. S. Porphyrins bearing mono or tripodal benzylphosphonic acid tethers for attachment to oxide surfaces. *J. Org. Chem.* **2004**, *69* (5), 1453−60.
(35) Qiu, W.; Burton, D. J. A facile and general preparation of α,α-difluoro benzylic phosphonates by the CuCl promoted coupling reaction of the (diethylphosphonyl)difluoromethylcadmium reagent with aryl lodides. *Tetrahedron Lett.* **1996**, *37*, 2745−2748.
(36) Balimane, P. V.; Han, Y. H.; Chong, S. Current industrial practices of assessing permeability and P-glycoprotein interaction. *AAPS J.* **2006**, *8* (1), E1−13.
(37) Gao, Z.; Johansen, E.; Eyers, S.; Thomas, C. L.; Noel Ellis, T. H.; Maule, A. J. The potyvirus recessive resistance gene, sbm1, identifies a novel role for translation initiation factor eIF4E in cell-to-cell trafficking. *Plant J.: Cell. Mol. Biol.* **2004**, *40* (3), 376−85.
(38) Leslie, A. G. W. Recent changes to the MOSFLM package for processing film and image plate data. *Joint CCP4 + ESF-EAMCB Newsl. Protein Crystallogr.* **1992**, 26.
(39) CCP4 (Collaborative Computational Project, No 4). The CCP4 suite: programs for protein crystallography. *Acta Crystallogr., D: Biol. Crystallogr.* **1994**, *50* (Pt 5), 760−3.
(40) Vagin, A.; Teplyakov, A. Molecular replacement with MOLREP. *Acta Crystallogr., D: Biol. Crystallogr.* **2010**, *66* (Pt 1), 22−5.
(41) Emsley, P.; Cowtan, K. Coot: model-building tools for molecular graphics. *Acta Crystallogr., D: Biol. Crystallogr.* **2004**, *60* (12), 2126−32.
(42) Murshudov, G. N.; Vagin, A. A.; Dodson, E. J. Refinement of macromolecular structures by the maximum-likelihood method. *Acta Crystallogr., D: Biol. Crystallogr.* **1997**, *53* (Pt 3), 240−55.